TERNARY PHASE EQUILIBRIA IN TRANSITION METAL-BORON-CARBON-SILICON SYSTEMS

PART II. TERNARY SYSTEMS

Volume XVII. Constitution of Ternary Ta-Mo-C Alloys

E. RUDY
ST. WINDISCH
C. E. BRUKL

FOREWORD

The research described in this report was carried out at the Materials Research Laboratory, Aerojet-General Corporation, Sacramento, California, under USAF Contract No. AF 33(615)-1249. The contract was initiated under Project No. 7350, Task No. 735001, and was administered under the direction of the Air Force Materials Laboratory, with Lt. P. J. Marchiando acting as Project Engineer, and Dr. Erwin Rudy, Aerojet-General Corporation, as Principal Investigator. Professor Dr. Hans Nowotny, University of Vienna, served as consultant to the project.

The project, which includes the experimental and theoretical investigations of ternary and related binary systems in the system classes Me_1-Me_2-C, Me-B-C, Me_1-Me_2-B, Me-Si-B and Me-Si-C, was initiated on 1 January 1964. An extension effort to this contract commenced in January 1966.

The phase diagram work on the ternary system described in this report was carried out by E. Rudy, St. Windisch, and C. E. Brukl. Assisting in the investigations were: J. Hoffman (metallographic preparations), J. Pomodoro (sample preparation), and R. Cobb (X-ray exposures and photographic work).

Chemical analysis of the alloys was performed under the supervision of Mr. W. E. Trahan, Quality Control Division of Aerojet-General Corporation. The authors wish to thank Mr. R. Cristoni for the preparation of the illustrations, and Mrs. J. Weidner, who typed the report.

The manuscript of this report was released by the authors August 1967. An abridged version of the report was submitted for publication in the Journal of the American Ceramic Society.

Other reports issued under USAF Contract AF 33(615)-1249 have included:

Part I. Related Binaries

Volume I.	Mo-C System
Volume II.	Ti-C and Zr-C Systems
Volume III.	Systems Mo-B and W-B
Volume IV.	Hf-C System
Volume V.	Ta-C System. Partial Investigations in the Systems V-C and Nb-C
Volume VI.	W-C System. Supplemental Information on the Mo-C System
Volume VII.	Ti-B System
Volume VIII.	Zr-B System
Volume IX.	Hf-B System
Volume X.	V-B, Nb-B and Ta-B Systems
Volume XI.	Final Report on the Mo-C System
Volume XII.	Revision of the Vanadium-Carbon and Niobium-Carbon Systems

Part II. Ternary Systems

Volume I.	Ta-Hf-C System
Volume II.	Ti-Ta-C System
Volume III.	Zr-Ta-C System
Volume IV.	Ti-Zr-C, Ti-Hf-C, and Zr-Hf-C Systems
Volume V.	Ti-Hf-B System
Volume VI.	Zr-Hf-B System
Volume VII.	Systems Ti-Si-C, Nb-Si-C, and W-Si-C
Volume VIII.	Ta-W-C System
Volume IX.	Zr-W-B System. Pseudo-Binary System TaB_2-HfB_2
Volume X.	Systems Zr-Si-C, Hf-Si-C, Zr-Si-B, and Hf-Si-B
Volume XI.	Systems Hf-Mo-B and Hf-W-B
Volume XII.	Ti-Zr-B System
Volume XIII.	Phase Diagrams of the Systems Ti-B-C, Zr-B-C, and Hf-B-C
Volume XIV.	The Hafnium-Iridium-Boron System
Volume XV.	Constitution of Niobium-Molybdenum-Carbon Alloys
Volume XVI.	The Vanadium-Niobium-Carbon System

Part III. Special Experimental Techniques

Volume I.	High Temperature Differential Thermal Analysis
Volume II.	A Pirani-Furnace for the Precision Determination of the Melting Temperatures of Refractory Metallic Substances

Part IV. Thermochemical Calculations

Volume I.	Thermodynamic Properties of Group IV, V, and VI Binary Transition Metal Carbides
Volume II.	Thermodynamic Interpretation of Ternary Phase Diagrams
Volume III.	Computational Approaches to the Calculation of Ternary Phase Diagrams.

This technical report has been reviewed and is approved.

W. G. RAMKE
Chief, Ceramics and Graphite Branch
Metals and Ceramics Division
Air Force Materials Laboratory

ABSTRACT

The ternary system tantalum-molybdenum-carbon was investigated by means of X-ray, melting point, DTA, and metallographic techniques on chemically and thermally characterized specimens; a complete phase diagram for temperatures above 1500°C was established.

The observed phase relationships are thermodynamically analyzed and the calculated temperature sections are found to be in good agreement with the experimental observations.

TABLE OF CONTENTS

LIST OF ILLUSTRATIONS

LIST OF ILLUSTRATIONS (Cont.)

LIST OF ILLUSTRATIONS (Cont.)

LIST OF TABLES

I. INTRODUCTION AND SUMMARY OF PREVIOUS WORK

A. INTRODUCTION

Continuing our studies of the high temperature phase relationships in binary and ternary systems of the refractory transition metals with carbon, boron, and silicon[1], we have now investigated the phase relationships in the Ta-Mo-C system. Particular attention was devoted to the examination of the possibility of obtaining stable, two-phase combinations of monocarbide and metal alloys for application in high temperature, abrasion-resistant composites, and for heat-resistant cutting tools. Previous work[2, 3] on combinations of group V and VI transition metals with carbon has shown that under certain thermodynamically controlled conditions, formation of a solid solution, or of two-phase equilibria, between the Me_2C-phases does not occur; and that two-phase equilibria between monocarbide and metal alloys are formed instead. Examples where such equilibria are present are in the alloy systems Nb(Ta)-Mo(W)-C; whereas, in the corresponding systems with vanadium, the subcarbides form continuous series of solid solutions.

Differences, however, do also exist between the niobium- and tantalum-containing systems; these differences become especially apparent in the temperature range above 2000°C: In the Nb-Mo-C system, the equilibrium: $(Nb, Mo)C_{1-x}(B1)$ + (Nb, Mo) remains stable up to solidus temperatures[5]; contrasting with this phase behavior, the subcarbides Ta_2C and W_2C become completely miscible above 2450°C. Because the relative stabilities of Mo_2C and W_2C are very similar, the metal-rich equilibria in the systems Nb-W-C and Ta-Mo-C will be governed, therefore, mainly by the relative stabilities of Ta_2C and Nb_2C; consequently, the temperature variation of the phase equilibria in the Ta-Mo-C ternary system is expected to be similar to that in the Ta-W-C system.

B. SUMMARY OF PREVIOUS WORK

The phase diagrams of the binary systems are well established. Tantalum and molybdenum are miscible in all proportions[6, 7], and the solidus temperatures vary almost linearly between the melting points of the constituents[7].

The complex phase relationships in the molybdenum-carbon system (Figure 1) have been only recently delineated in detail[8], although the intermediate phases had been structurally characterized previously. Three intermediate phases, Mo_2C, η-MoC_{1-x}, and α-MoC_{1-x} occur in the system. The latter two are high temperature phases and can be retained only by severe quenching. The subcarbide, Mo_2C, exists in several states of sublattice order and shows a complex transformation behavior: Substoichiometric (< 32.5 At.% C) alloys undergo a homogeneous (single-phased) order-disorder transition in the vicinity of 1400°C. Stoichiometric and hyperstoichiometric alloys, on the other hand, cannot exist in the ordered state; upon cooling through the critical temperature range, they disproportionate into a hypostoichiometric alloy,

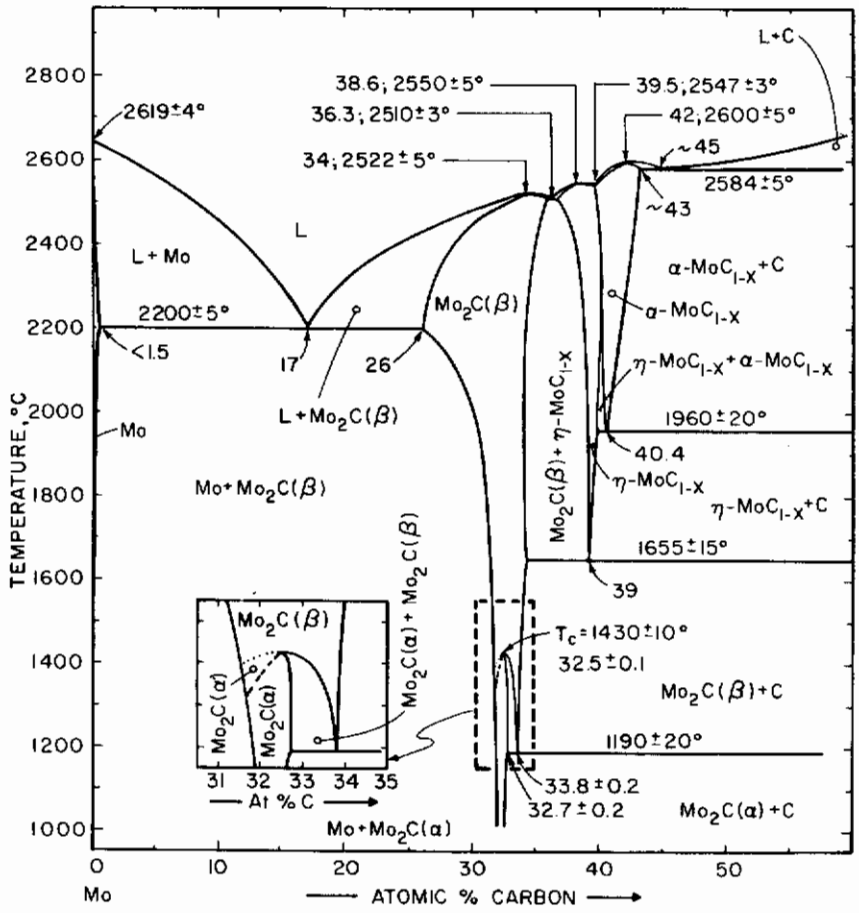

Figure 1. Constitution Diagram for the Mo-C System.

(After E. Rudy et al., 1967. Temperature error figures refer to the reproducibility of the measurements).

which is ordered, and a hyperstoichiometric alloy which is disordered and decomposes at somewhat lower temperatures in a eutectoid (pseudomonotectoid) reaction into the ordered modification and free graphite. In addition to the ordering reaction, the hexagonal close-packed metal host lattice undergoes a slight distortion in the transformation process. Structural details as well as lattice parameters for the molybdenum carbides are compiled in Table 1.

The most recent phase diagram[12] of the tantalum-carbon system is shown in Figure 2. The system contains an extremely refractory, cubic monocarbide and a peritectically decomposing, hexagonal subcarbide. The ordered, low temperature modification of Ta_2C[11] transforms at temperatures between 2100 and 2200°C[12] into another modification, which is

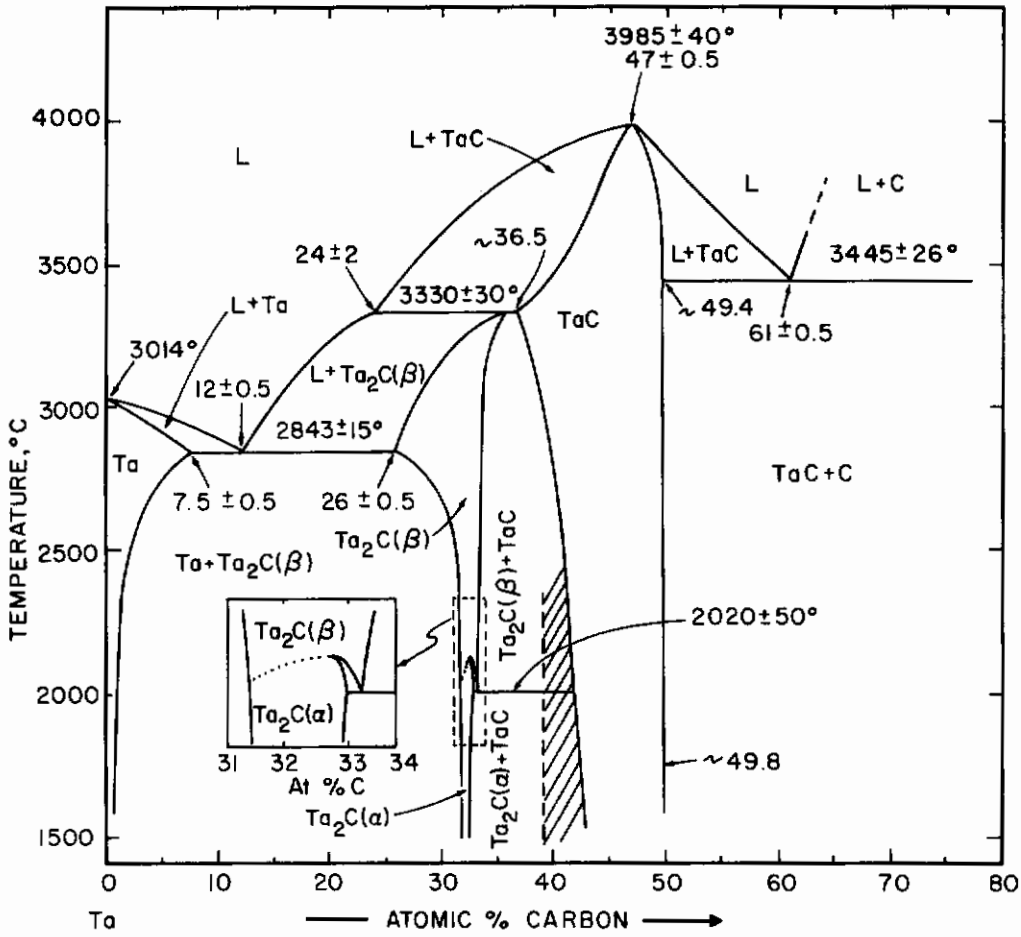

Figure 2. Constitution Diagram for the Tantalum-Carbon System. Shaded Area Shows the Range of the Metastable ζ-Phase.

(After E. Rudy, 1966. Temperature figures include mean value and estimated overall uncertainty).

Table 1. Structure and Lattice Parameters of Molybdenum and Tantalum Carbides

Phase	Structure	Lattice Parameters, Ångstrom
Mo_2C	1. T<~1400°C: Orthorh., D_{2h}^{14}-Pbcn. (C-Sublattice Ordered)	a=4.724; b=6.004; c=5.19 (9) a=4.733; b=6.042; c=5.202 (8) at 32.5 At% C
	2. T>~1400°C: Hex., Approaching L'3-type (no long range order in carbon sublattice)	a=2.990; c=4.730 at 30 At%C a=3.010; c=4.778 at 34.4 At% C (8) (alloys quenched from 2000°C)
η-MoC_{1-x}	Hex., D_{6h}^{4}	a=3.006; c=14.64 (10) a=3.010; c=14.64 at 39 At%C (8)
α-MoC_{1-x}	Fcc., B1-type	a=4.266 at 39.7 At% C a=4.281 at 43 At% C (8)
Ta_2C	1. T<2000-2150°C: Hex., C6-type	a=3.103; c=4.938 at 33 At%C (11) a=3.100; c=4.931 at 31.5 At%C a=3.102; c=4.940 at 33 At% C (12)
	2. T>2150°C: Hex., L'3-type (no long range order in carbon sublattice)	L'3-type cannot be retained by quenching; parameters comparable to those of the ordered modification.
TaC	Fcc., B1-type	a=4.411 at 42.5 At% C a=4.4545 at ~50 At% C (13)

characterized by the absence of long range order in the carbon sublattice. With the exception of the displacive transformation, which is absent in Ta_2C, the transformation characteristics are similar to that of Mo_2C. Another phase, ζ, reported to occur in the vicinity of 40 At.% carbon[13], was indicated to be only metastable[12, 14]; the latter viewpoint, however, was disputed in more recent work[15]. A compilation of structural data as well as of lattice parameters for the tantalum carbides is also contained in Table 1.

Earlier investigations of ternary Ta-Mo-C alloys include the establishment of extensive solid solubility along the section $TaC-Mo_2C$[16], and of an isothermal section of the system at 1800°C[17].

II. EXPERIMENTAL

A. STARTING MATERIALS AND ALLOY PREPARATION

The elemental powders, as well as specially prepared master alloys of Ta_2C, TaC, and Mo_2C, served as starting materials for the preparation of the experimental specimens.

Tantalum (99.9% pure) was purchased as powder from Wah Chang Corporation, Albany, Oregon. The impurities, in ppm, were as follows: C-140, Nb-100, O-280, sum of other contaminants-<300. A lattice parameter of a = 3.303 Å is consistent with the lattice spacings for high purity tantalum given in Pearson[18].

The molybdenum powder (Wah Chang Corp., Glen Cove, New York) had the following impurities after an additional hydrogen treatment at 1000°C (contents in ppm): O-160, Si-<180, Nb-<180, N-<20, C-190, sum of Fe, Ni, Co-<110, and sum of other metallic impurities (Al, Cr, Cu, Mg, Mn, Pb, Sn, W, Ti)-<600. A lattice parameter of $a = 3.1474 \pm 0.0002$ Å was obtained from an exposure with Cu-K_α radiation.

The spectrographic grade graphite powder was purchased from Union Carbide Corporation, Carbon Products Division. The total impurity content was below 2 ppm.

Tantalum monocarbide was purchased as 10 micron powder from Wah Chang Corporation, Albany, Oregon. The powder was acid-leached to remove soluble constituents and high-vacuum degassed (2 hrs at 4×10^{-6} Torr at 2200°C) to eliminate volatile contaminants. The lattice parameter of the purified product was $a = 4.4560 \pm 0.0003$ Å. The monocarbide had a total

carbon content of 6.15$_6$ Wt%, of which 0.04 Wt% were present in elemental form. The following impurities were found in the processed material (in ppm): Ti-400, Nb-150, Y-200, O-<20, N-<10, H-not detected, Cr-<25, Co-40, Fe-<70, sum of B, Mg, Mn, Ni, Pb, Si and Sn-<50.

Ditantalum carbide and Mo_2C were prepared by reacting the carefully blended and cold-compacted mixtures of the metal powders and graphite in a graphite-element furnace under a vacuum of better than 2×10^{-5} Torr. The thermal treatments were four hours at 2000°C for Ta_2C, and 2 hours between 1600 and 1960°C for Mo_2C. The reaction lumps were crushed and ball-milled to a grain size smaller than 60 microns, and cobalt pick-up from the hard metal lined jars was removed by acid-leaching.

The Ta_2C-powder had a total carbon content of 33.0 At.%, and lattice parameters of $a = 3.102$ Å, and $c = 4.938$ Å. The combined contents of oxygen and nitrogen were less than 140 ppm.

The dimolybdenum carbide powder contained 32.7 ± 0.2 At.% carbon, of which 0.2 At% were present as elemental graphite. Other contaminants included (in ppm): O-70, N-<10, and Si-<100.

The majority of the experimental samples was prepared by short duration (2 to 5 minutes) hot pressing[19] of the hand mixed powders in graphite dies. The hot pressing temperatures varied between 1600°C and 2500°C. After hot pressing, the thin, carburized surface zones were removed by grinding and the samples then subjected to further heat treatments. Equilibration treatments for the investigation of the solid state sections of the system were 1500°C, 1800°C, 2200°C, and 2500°C. The heat treatments were carried out in a tungsten-mesh element furnace, using either vacuum (5×10^{-6} Torr) or, for treatments above 2000°C, high purity helium at ambient pressure. The variation of certain equilibria towards still higher temperatures was studied on alloys which were equilibrated in the Pirani-furnace[20] and then radiation-cooled or quenched in tin. For metallographic purposes, a piece of each alloy was also arc-melted under helium using a non-consumable tungsten electrode. For melting and DTA-experiments, excess metal-containing

specimens were prepared by cold-pressing the powdered ingredients; these samples were used in the as-pressed state.

B. DETERMINATION OF MELTING TEMPERATURES

The solidus temperatures of approximately 140 alloys were measured using the method devised by M. Pirani and H. Alterthum[21]. In this technique, a small sample bar is resistively heated between two water-cooled copper electrodes to the temperature of the phase change. The temperature is measured with a disappearing-filament type pyrometer aimed through a quartz port in the furnace at a small black body hole (0.6 to 1 mm in diameter, 4 to 6 mm deep) located in the center of a narrowed portion of the specimen. The specimen clamping arrangement used for the melting point determinations is shown in Figure 3. Further design details of the apparatus used in this laboratory, as well as temperature calibration and correction data, have been published elsewhere[20] and therefore need not be described at length here.

In the measurements, the specimens were held under slight compression (50-100 gr) and heated in vacuum to temperatures between 1800 and 2300°C until no further degassing was noticeable. The furnace chamber was then pressurized with high purity helium to approximately 2 atmospheres, or to six atmospheres for high melting monocarbide alloys. The latter measure was taken to retard the preferential loss of carbon from the specimens. The temperature of the specimens was then gradually raised until liquid formation was either noticed visually or detected by the occurrence of a thermal arrest.

Post-experimental analysis of the alloys indicated that the carbon losses during melting were very nominal, and the analyzed compositions agreed, as a rule, to within one atomic percent of the weighed-in compositions.

Oxygen and nitrogen contamination of the processed alloys, determined on a random selection basis on a number of alloys, was less than

40 ppm in each alloy studied; the possible effect of these contaminants upon the measured phase equilibria is judged to be negligible.

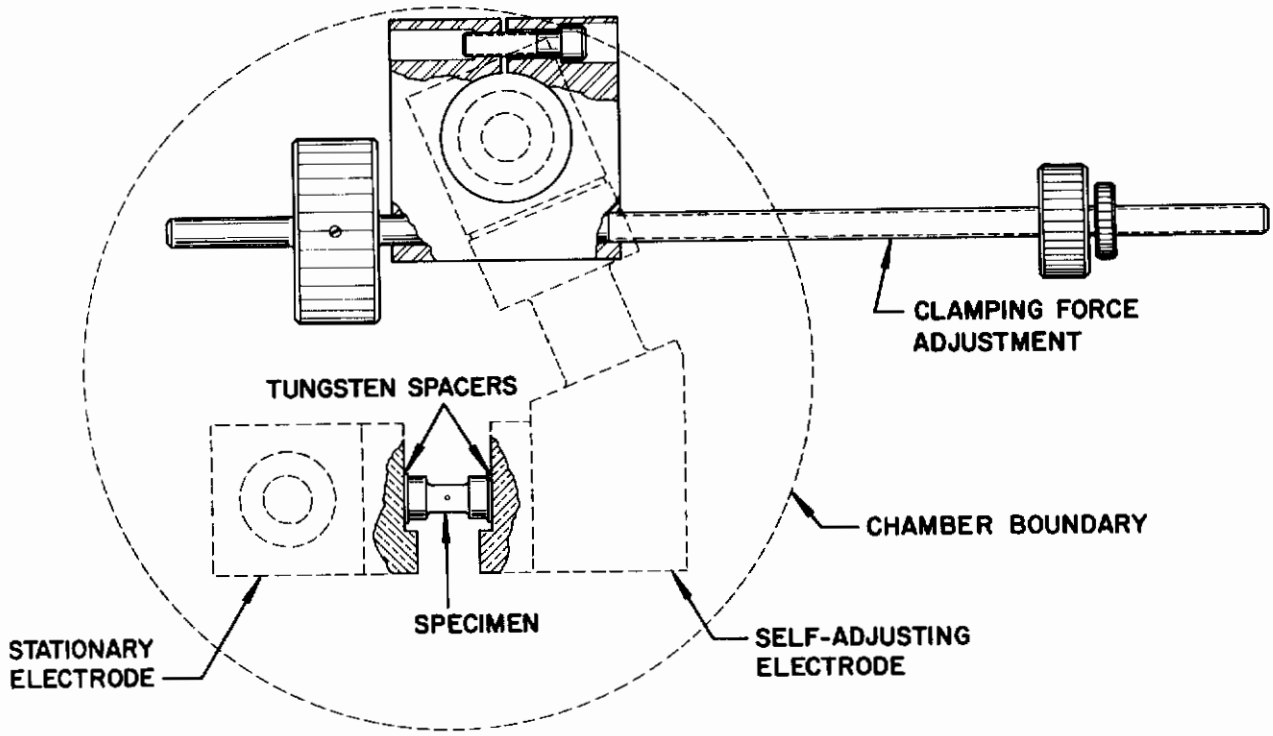

Figure 3. Specimen Clamping Arrangement in the Melting Point Furnace.

C. DIFFERENTIAL AND DERIVATIVE THERMAL ANALYSIS

With tantalum monocarbide as well as annealed graphite as comparison standards, and graphite as a container material, the thermal behavior of a total of 45 ternary alloys was studied by differential thermo-analytical techniques. As a result of the limitations imposed by the choice of the container material, these measurements had to be restricted to temperatures below the monocarbide + graphite solidus. Fortunately, however, tantalum carburizes preferentially,and thus a refractory interface between the sample surface and the graphite container is formed; the measurements,

therefore, could be extended well into the melting range of metal-rich (< 36 At.% C) alloys. Nevertheless, in order to ensure that no eventual solid state reactions in the subsolidus range of the monocarbide solutions remained undetected, four monocarbide alloys, having carbon contents of 45 atomic percent, were run in the Pirani furnace. The thermal behavior of the specimens was studied between 1000°C and the respective solidus temperatures, using the derivative thermal analysis apparatus described in an earlier paper[8]. However, since no further reactions were detected, no additional mention of these experiments will be made.

D. METALLOGRAPHIC, X-RAY, AND CHEMICAL ANALYSIS

For microscopic studies, the specimens were mounted in a mixture of diallylphtalate and lucite-coated copper powder and preground on silicon-carbide paper. The ground surfaces were then polished using a slurry of Linde "B" alumina (0.3μ) in a 5% chromic acid solution. The etching procedures varied with the alloy compositions and are described in Table 2.

Carbon in the alloys was determined in the well-known manner by combustion of the powdered specimens in oxygen and subsequent conductometric analysis of the resulting gas-mixture. For the determination of free graphite, the powdered alloys were first dissolved in a mixture of nitric and hydrofluoric acid and the residual graphite analyzed by combustion as described above. The reproducibility of the results was usually better than 0.02 Wt.%.

Oxygen and nitrogen were hot-extracted in a gas-fusion analyzer, whereas low level metallic impurities were determined in a semi-quantitative manner spectrographically.

Power diffraction patterns were prepared from all experimental alloys and the film strips evaluated with respect to number, structure, and lattice dimensions of the phases. The tie line distribution in the various two-phase fields and the location of the vertices of the three-phase equilibria were determined by lattice parameter measurements.

Table 2. Etching Procedures for Tantalum-Molybdenum-Carbon Alloys

Composition Range	Etching Procedures
$Ta-Ta_{0.65}C_{0.35}-Ta_{0.25}M_{0.75}$	Electroetched in 0.5% aqueous oxalic acid solution
$Ta_{0.65}C_{0.35}-Ta_{0.55}C_{0.45}-$ $-Mo_{0.55}C_{0.45}-Mo-Ta_{0.25}Mo_{0.75}$	Swab-etched with 20% Murakami's solution
Alloys containing more than 45 At% C	1. Preconditioning of sample surfaces with a 10% aqueous solution of a mixture consisting of 6 parts concentrated HNO_3 and 4 parts HF. 2. Preferential grain boundary etching with 20% Murakami's solution. 3. Re-treatment with the acid-solution (1) to remove staining caused by Murakami's solution.

III. RESULTS

A. THE BINARY SYSTEM MOLYBDENUM-TANTALUM

Melting temperatures were determined on six binary alloys; each sample was run in duplicate. The measured solidus temperatures closely follow the data determined earlier by G.A. Geach and D. Summers-Smith[7] (Figure 4); the lattice parameters, determined on the annealed melting point samples, also agree well with previous data (Figure 5).

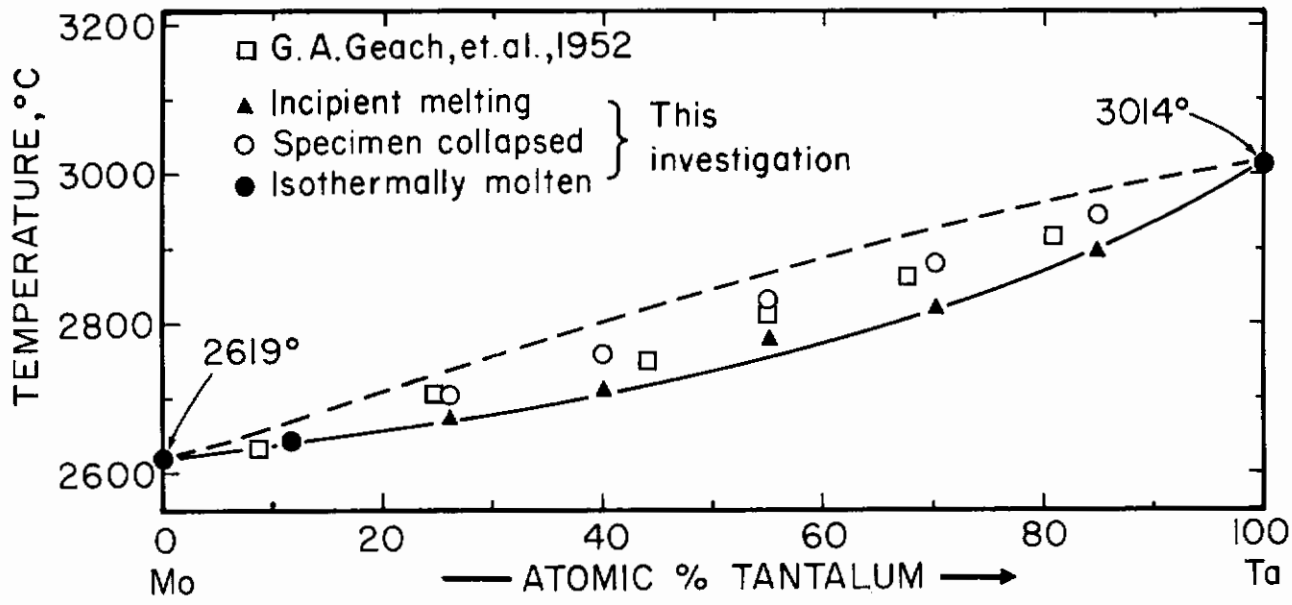

Figure 4. Melting Temperatures of the Tantalum-Molybdenum Solid Solution.

B. TERNARY Ta-Mo-C ALLOYS

1. Phase Equilibria in the Temperature Range from 1500-1800°C

The qualitative phase evaluation of the alloy series equilibrated at 1800°C yielded the phase distribution shown in Figure 6. At this temperature, the maximum molybdenum exchange in tantalum monocarbide is approximately 87 At%. This exchange is also verified by lattice parameter measurements (Figure 7).

Bound carbon in the monocarbide solid solution decreases with increasing molybdenum content and reaches a defect concentration of approximately 4 atomic percent at the vertex of the three-phase equilibrium: $(Ta, Mo)C_{1-x}$-ss + η-MoC_{1-x}-ss + graphite. The solid solubility in η-MoC_{1-x} is very small, and the phase is terminated by a three phase equilibrium: η-MoC_{1-x}-ss + $(Ta, Mo)C_{1-x}$-ss + Mo_2C-ss in the ternary.

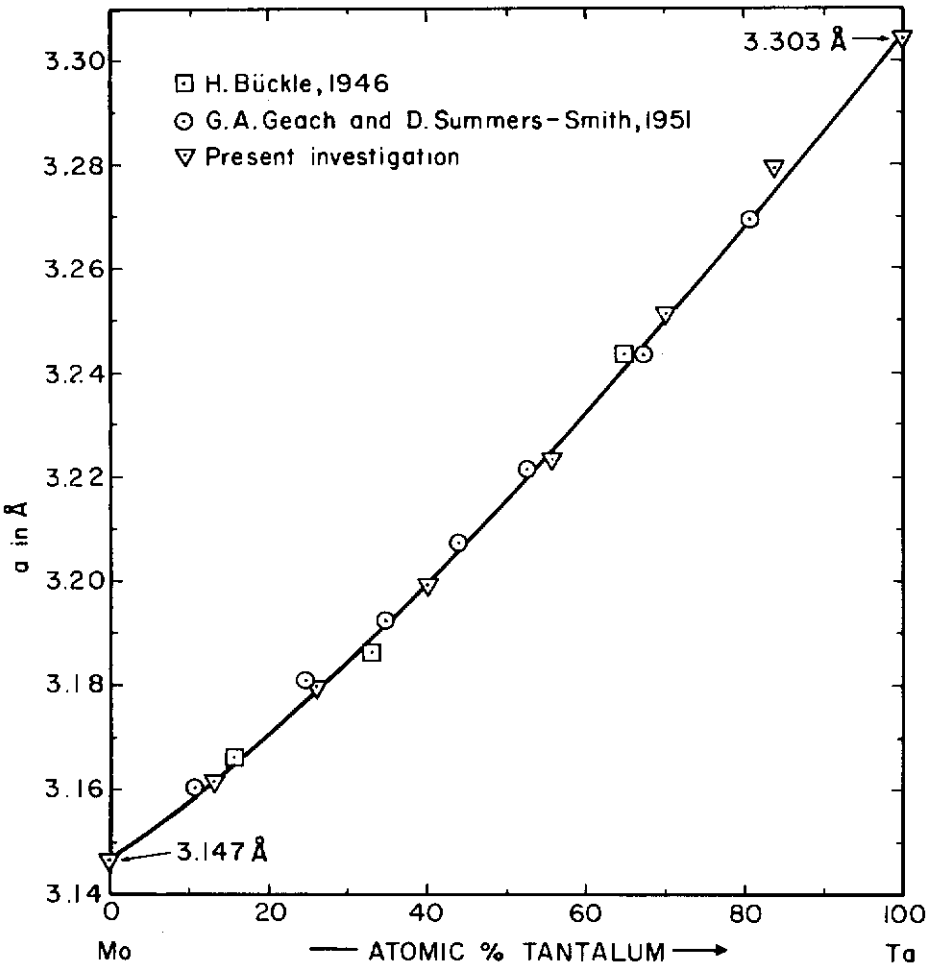

Figure 5. Lattice Parameters of the Tantalum-Molybdenum Solid Solution.

The maximum metal exchanges in the subcarbides are: 12 At% Mo in Ta_2C (a = 3.098 Å; c = 4.910 Å at the three phase boundary, as compared to a = 3.10$_2$ Å; c = 4.940 Å for Ta_2C and 40 At% Ta in Mo_2C (a = 3.038 Å; c = 4.797 Å for the terminal solid solution, as compared to a = 2.992, c = 4.733 Å for the binary Mo_2C). Both subcarbide solid solutions are terminated by three-phase equilibria in the ternary, and the monocarbide solution forms a two-phase equilibrium with the metal phase.

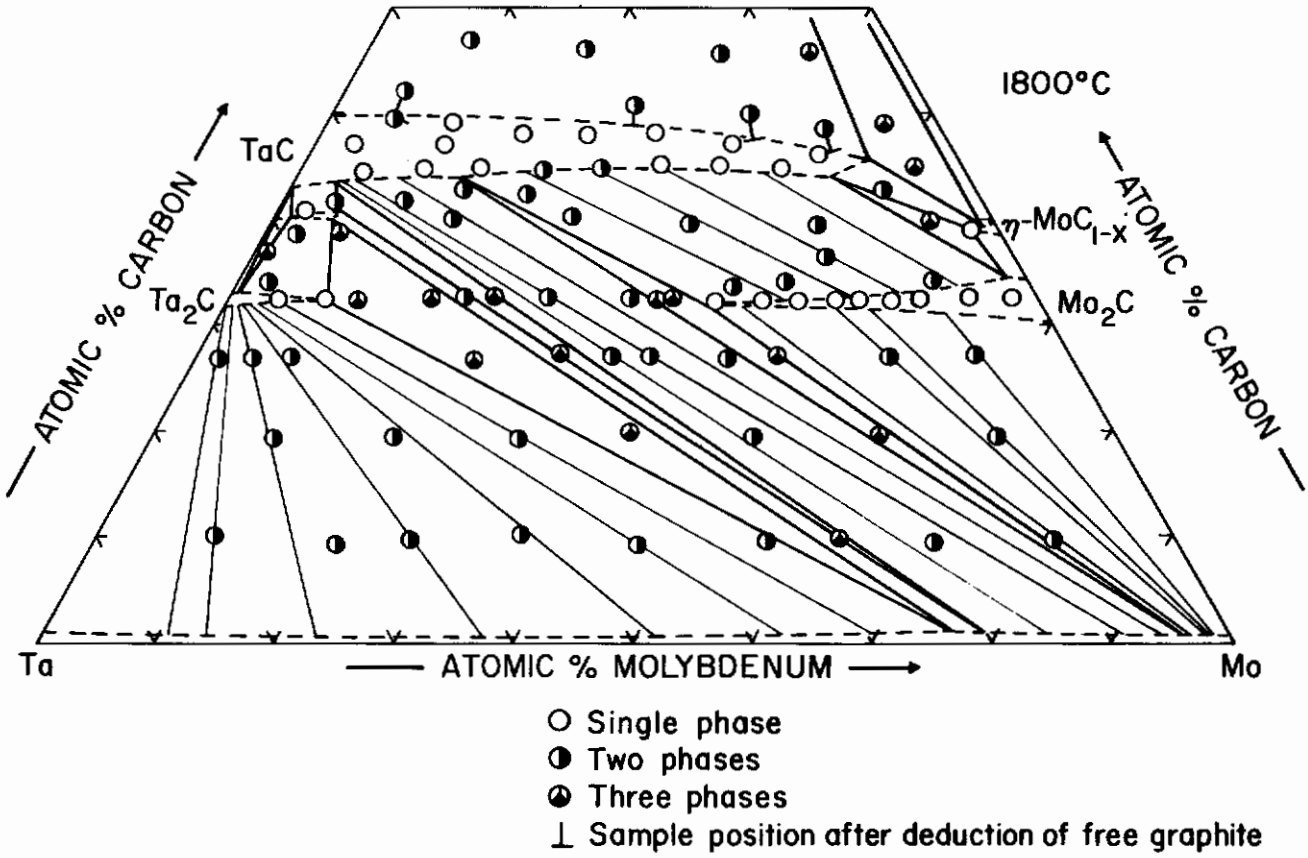

Figure 6. Qualitative Phase Evaluation of Ta-Mo-C Alloys After Equilibration at 1800°C.

An interesting feature in the ternary system concerns the apparent stability increase of the binary ζ-Ta,C-phase by molybdenum. The phase was present in practically pure form in alloys containing approximately 40 At% carbon and between 2 and 5 At% molybdenum (Figure 6); still smaller molybdenum contents invariably resulted in increased amounts of tantalum monocarbide and Ta_2C, whereas, at somewhat higher molybdenum concentrations, phase mixtures consisting of metal, monocarbide, and ζ-phase are found. Finally, an alloy Ta-Mo-C (48-10-42 At%) consisted only of monocarbide and subcarbide. The presence of the ζ-phase was observed in alloys containing as little as 10 At% carbon, and the relative proportion of the phases

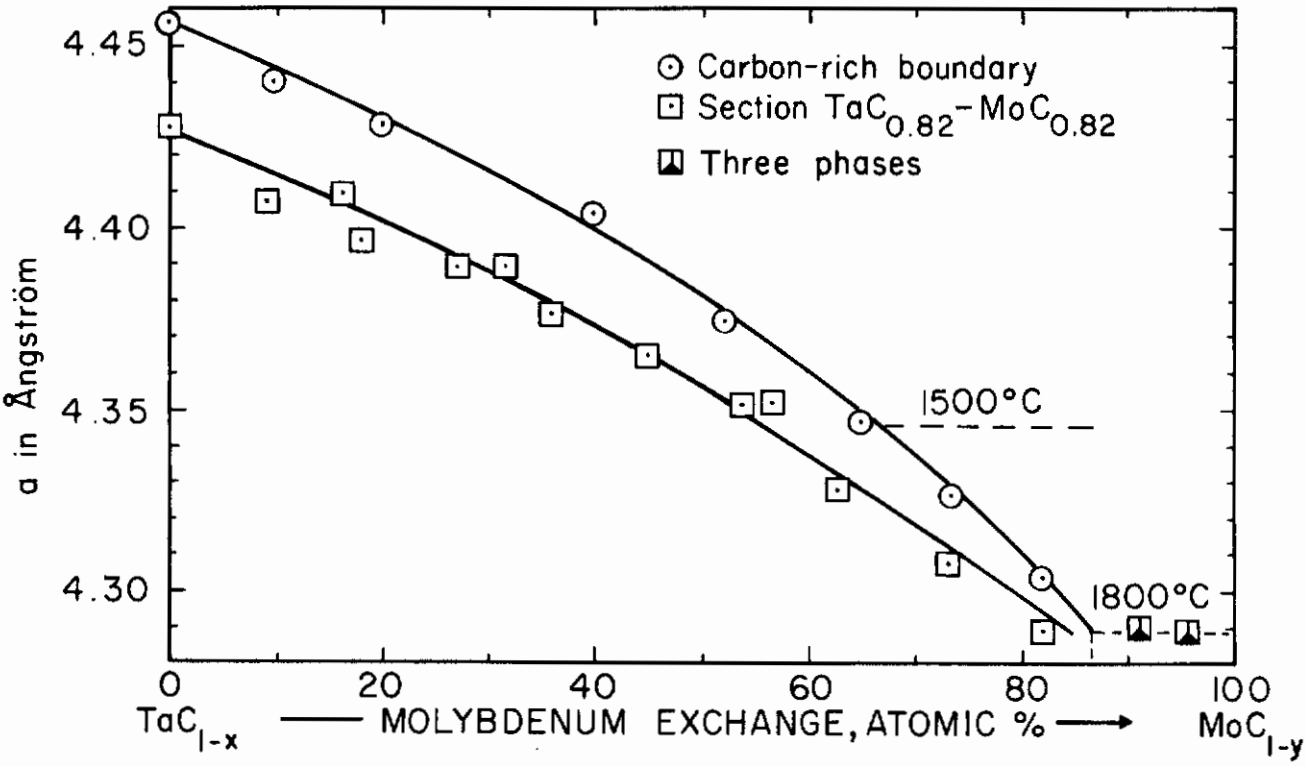

Figure 7. Lattice Parameters of the Monocarbide Solid Solution in 1800°C-Equilibrated Alloys.

present in ζ-containing alloys did not change after annealing for 320 hrs at 1800°C. Based upon these results, as well as on the additional observation that the two- and three-phase equilibria between ζ and the monocarbide, the subcarbide, and the metal solid solution, could be reproduced at all temperatures between 1500°C and 2000°C, it was concluded that the ζ is a stable, ternary phase.

As to be expected from a comparison of the thermodynamic stability of molybdenum and tantalum carbides, the swing of the tie lines in the two phase fields: metal + subcarbide, metal + monocarbide, and subcarbide + monocarbide phase (Figure 6) shows a pronounced enrichment of tantalum in the higher carbon-containing phases.

The gross features of the phase relationships found at 1500°C are very similar to those at 1800°C. The mutual metal exchanges in the subcarbide phases and the homogeneity range of the monocarbide solid solution are somewhat smaller, and the swing of the tie lines becomes more extreme than at 1800°C. The respective solubilities at 1500°C are: 8 Mole% Mo_2C in Ta_2C, 34 Mole% Ta_2C in Mo_2C, and 73 Mole% MoC_{1-x} ($a = 4.346$ Å) in tantalum monocarbide ($a = 4.456$ Å). The results of the experimental investigations at 1500°C have been incorporated into the corresponding isothermal section of the system presented in a later section of this report.

2. Phase Equilibria at High Temperatures

Solid solution formation between TaC and α-MoC_{1-x} becomes complete above 1960°C, the eutectoid decomposition temperature of the cubic molybdenum carbide. This fact is evidenced by the X-ray results obtained from quenched alloys (Figure 8), but especially by differential-thermoanalytical studies on alloys located close to the molybdenum-carbon binary (Figure 9). The high decomposition rates of the binary molybdenum carbides are greatly reduced by substitution of tantalum, and alloys containing more than approximately 10 atomic percent tantalum are retained single-phased by ordinary furnace (radiation) cooling. This behavior was independently confirmed by microscopic examination of moderately rapidly (2°- 20°C/sec) cooled alloys in which the typical decomposition structures were observed only at low tantalum contents (Figure 10); alloys higher in tantalum were single-phased.

In the metal-rich region of the ternary system, the phase equilibria change considerably in the temperature range from 2000 to 2250°C. An alloy series located along the section Ta_2C-Mo_2C, which was equilibrated at, and quenched from 2100°C (Figure 11) still showed the existence of the two-phase equilibrium: metal + monocarbide. On the other hand, however, two other alloy series quenched from approximately 2250 and 2500°C, showed complete solid solution formation between the subcarbides (Figures 11 and 12). It is known[8], that the parameters of the subcarbides are affected

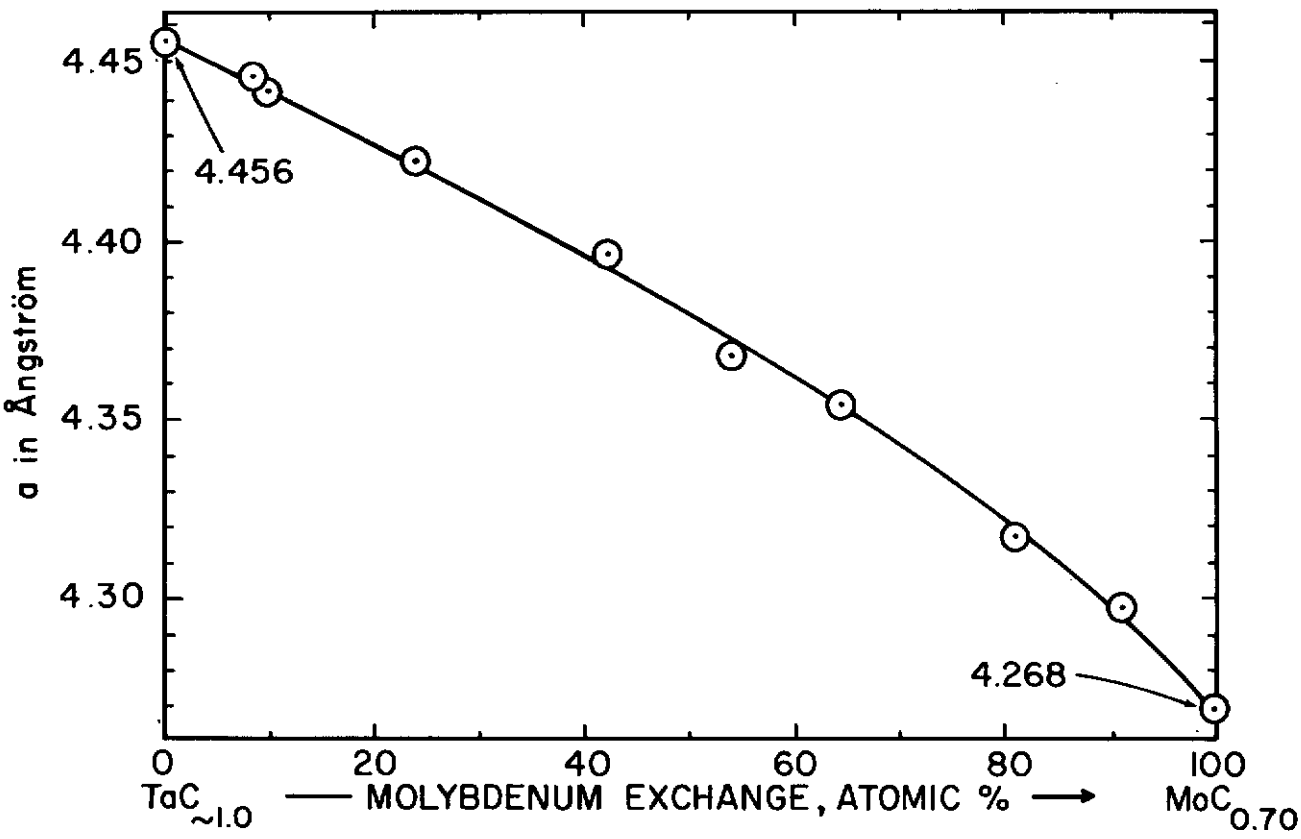

Figure 8. Lattice Parameters of the Cubic (B1) Monocarbide Solid Solution Along the Section TaC-$MoC_{0.70}$.

(Alloys Quenched from 2500°C).

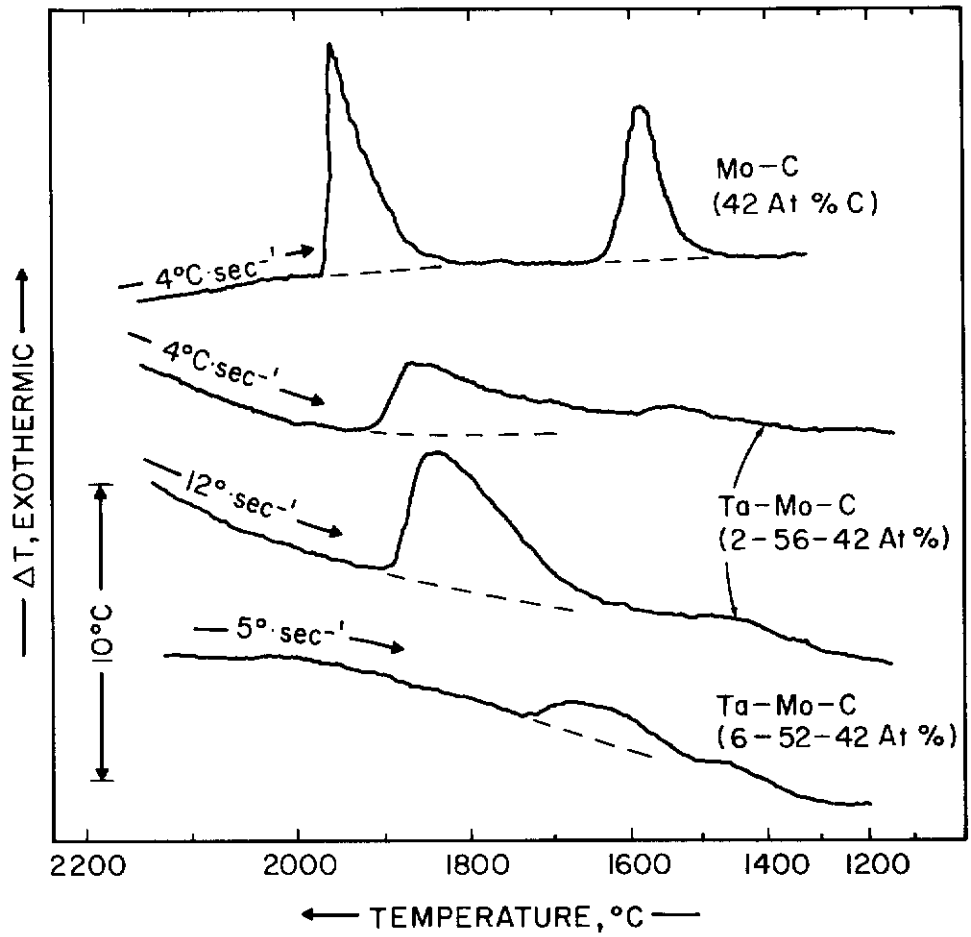

Figure 9. DTA-Thermograms (Cooling) of a Binary Mo-C Alloy (Top) and of Molybdenum-Rich Ta-Mo-C Alloys (Lower Curves) Located in the Concentration Domain of the Monocarbide Phase.

Top Curve: Decomposition of the α-MoC_{1-x} and η-MoC_{1-x} Phases at 1960°C and 1650°C, Respectively.

Lower Curve: Decomposition of the Monocarbide Solid Solution at Small Tantalum Concentrations.

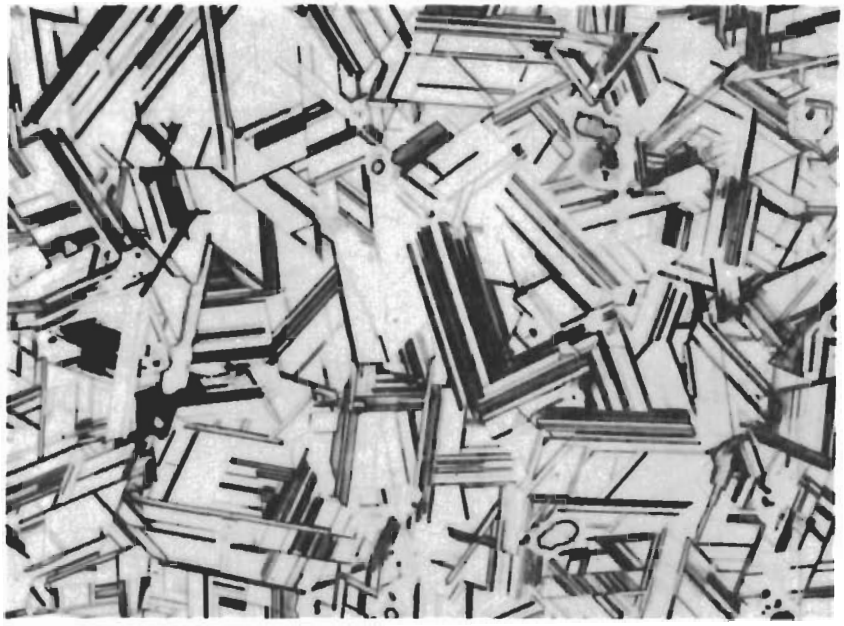

Figure 10. Ta-Mo-C (3-56-41 At%), Equilibrated at 2400°C and Cooled at 10°C per Second. X400

Decomposition Structure of the Monocarbide.

X-Ray: Monocarbide, η-MoC_{1-x}, and Dimolybdenum Carbide Solid Solution.

by the state of the sublattice order, in addition, since the speed of the order-disorder transformation depends upon the tantalum-molybdenum exchange, it is reasonable to assume that the relatively large scatter in the lattice parameter-concentration data shown in Figure 12 probably is to be attributed to differences in the degrees of order in the alloys following the quenching treatment.

The disproportionation of the subcarbide solid solution, even at the critical composition, occurs comparatively slowly, and cooling rates in excess of 10°C per second are usually sufficient to retain the alloys single-phased (Figure 13).

Apart from the effect of the relative metal concentrations, the decomposition was also found to be influenced by the presence of

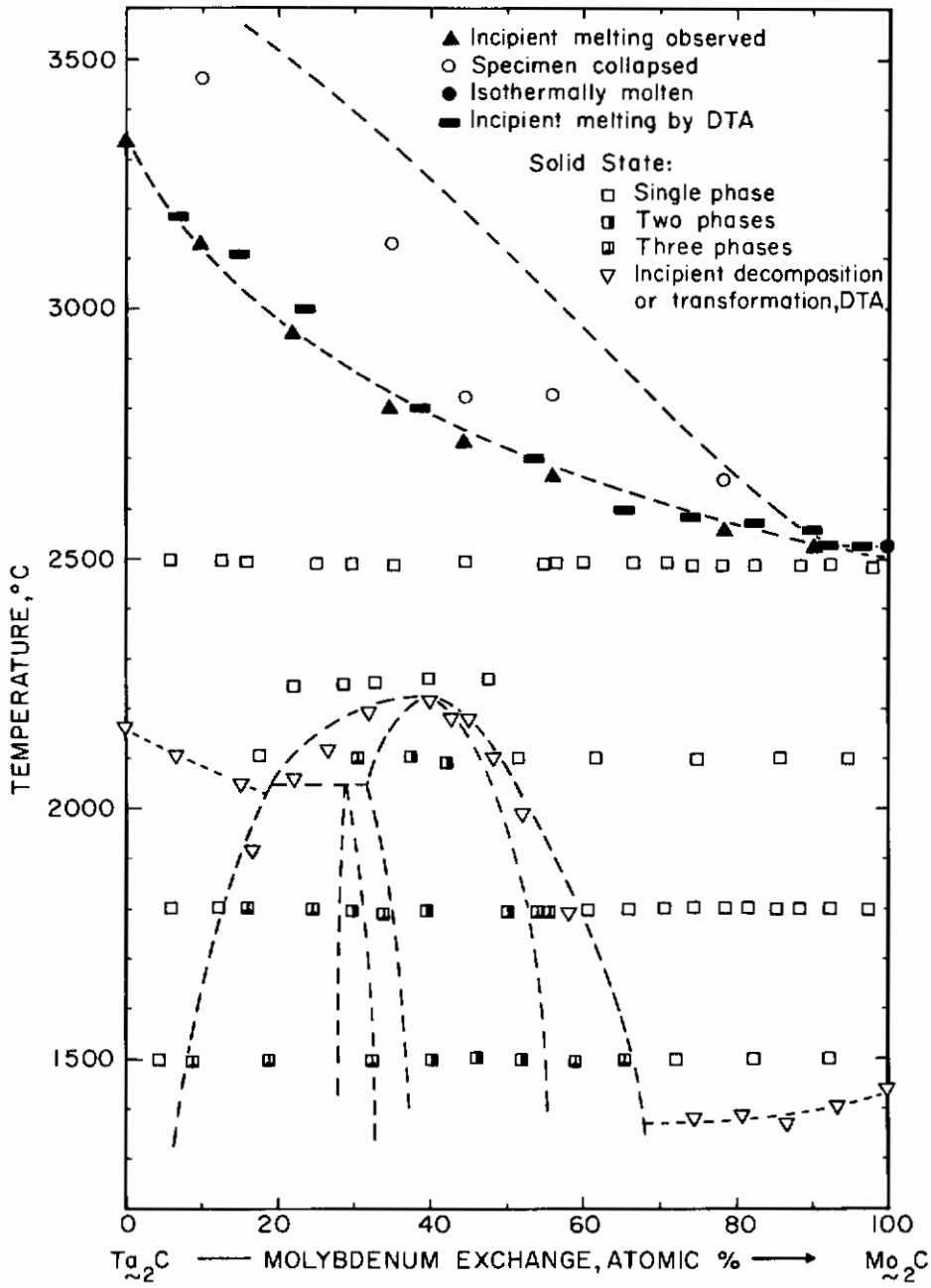

Figure 11. Melting and Qualitative Phase Evaluation of Alloys on the Section $Ta_{\sim 2}C$-$Mo_{\sim 2}C$.

Alloy Series at 1500°C Furnace-Cooled, All Others Quenched.

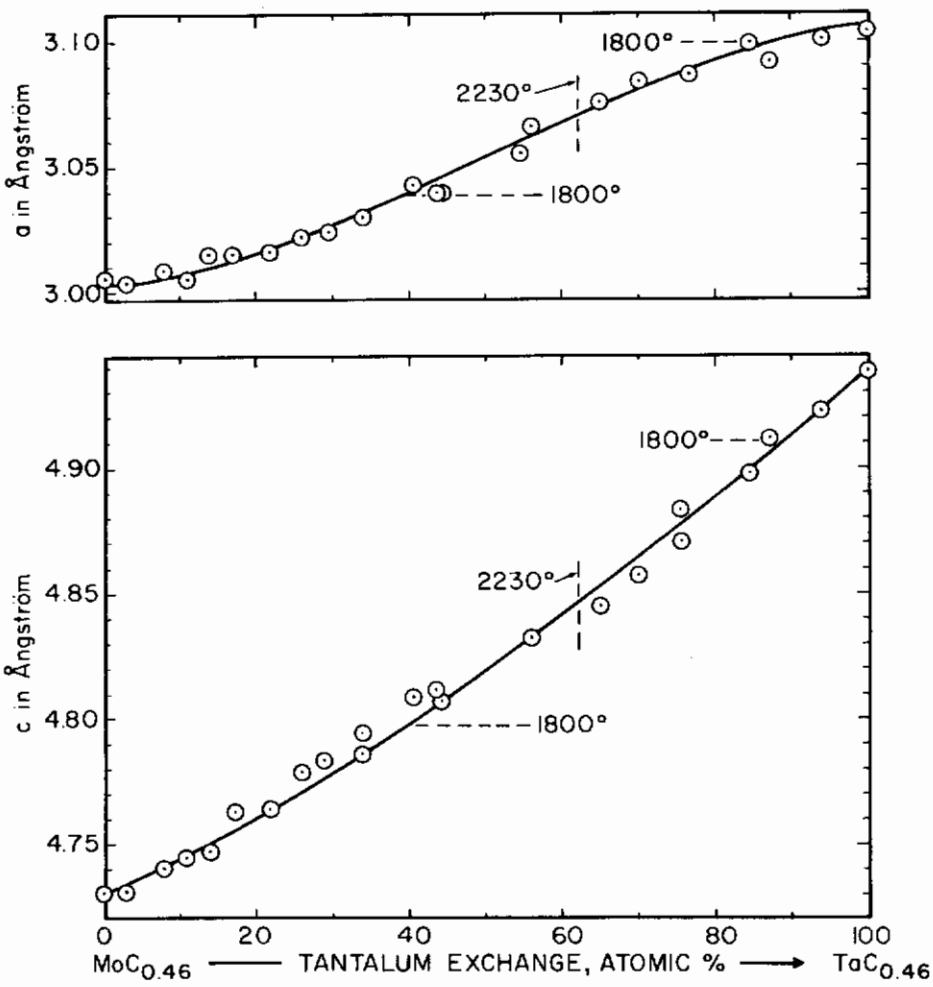

Figure 12. Lattice Parameters of the $(Ta, Mo)_2C$ Solid Solutions.

(Alloys Quenched from 2500°C, Parameters Based on Indexing According to the L'3-Type)

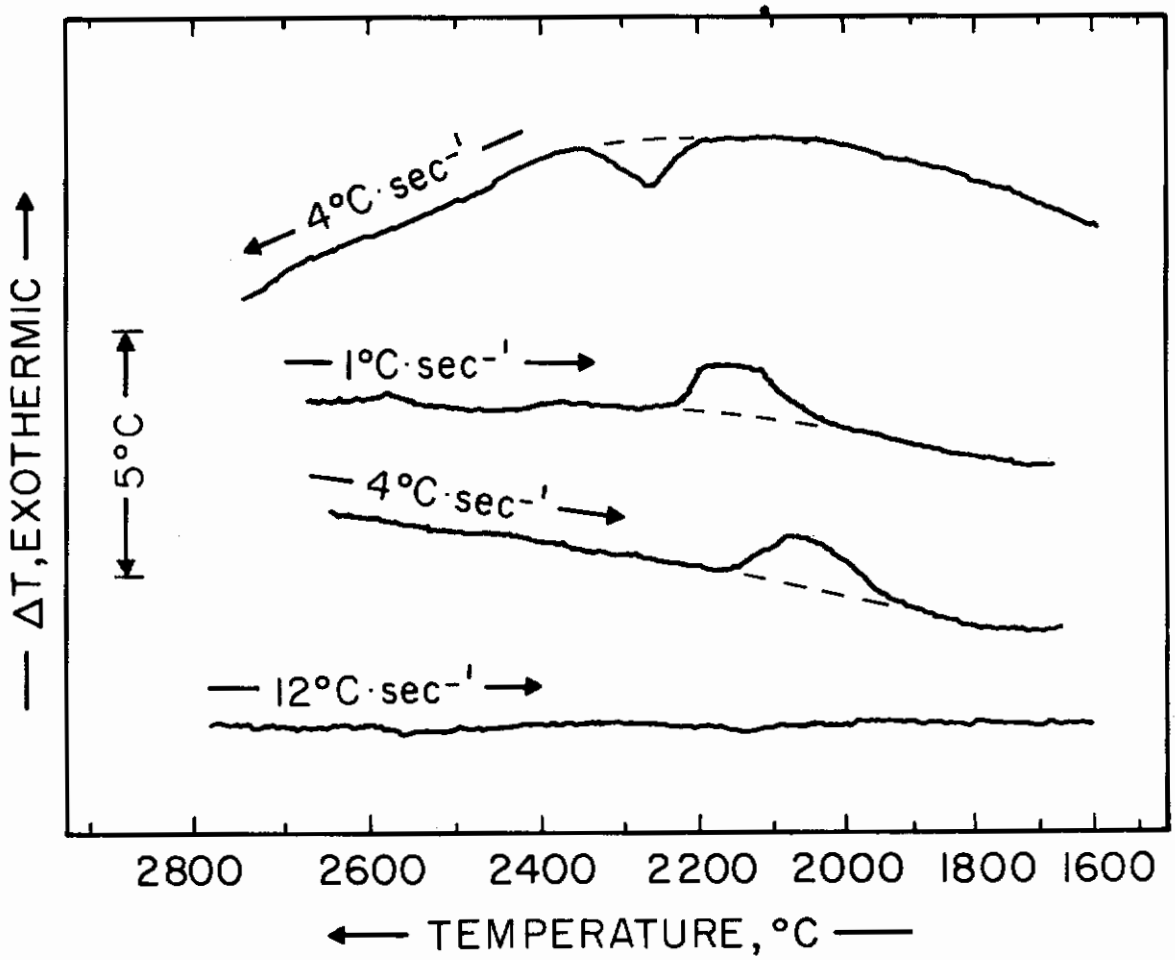

Figure 13. DTA-Thermograms of a Ta-Mo-C (41.6-25-33.4 At%) Alloy, Showing the Rate-Dependence of the Subcarbide Decomposition.

other phases and generally proceeded more rapidly in excess metal-containing alloys (Figure 14). This leads one to suspect that nucleation of the metal phase in the homogeneous subcarbide phase might be the rate-determining step. This supposition receives additional support from the microscopic observation that grain-boundary metal invariably served as the nucleation center for the decomposition reaction. From these grain boundaries the reaction then proceeds towards the center of the grains until all of the subcarbide

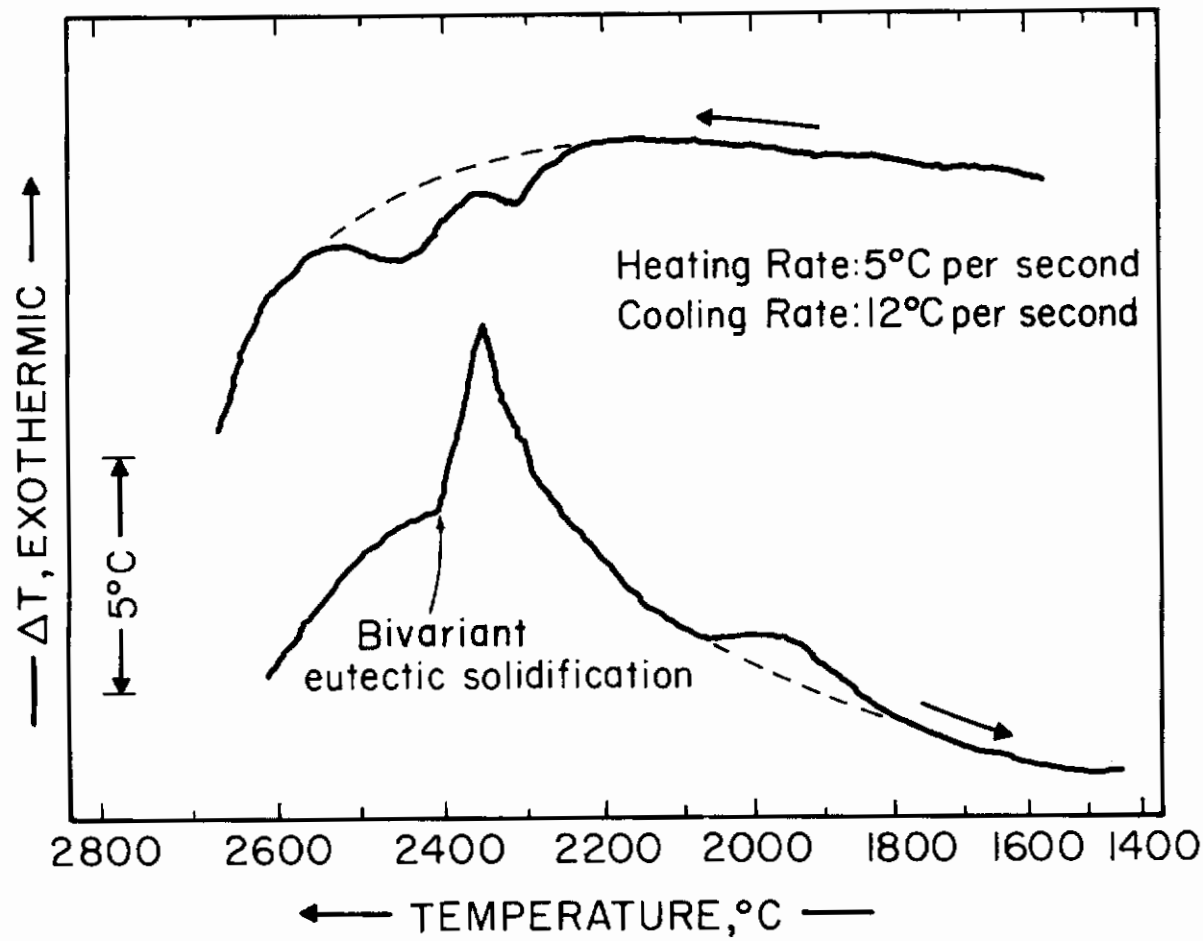

Figure 14. DTA-Thermogram of a Ta-Mo-C (43-28-29 At%) Alloy, Showing the Bivariant Melting and Solidification Along the Metal-Rich Eutectic Trough, and the Disproportionation of the $(Ta, Mo)_2C$ Solid Solution.

phase is decomposed (Figures 15, 16). The resulting decomposition structure is lamellar and consists of alternate layers of metal and monocarbide. Stemming from a nucleation and growth reaction, the lamellae spacing is markedly dependent upon the temperature at which the decomposition process is allowed to take place; if formed at temperatures below 2100°C, the unannealed structure usually cannot be resolved in the light microscope.

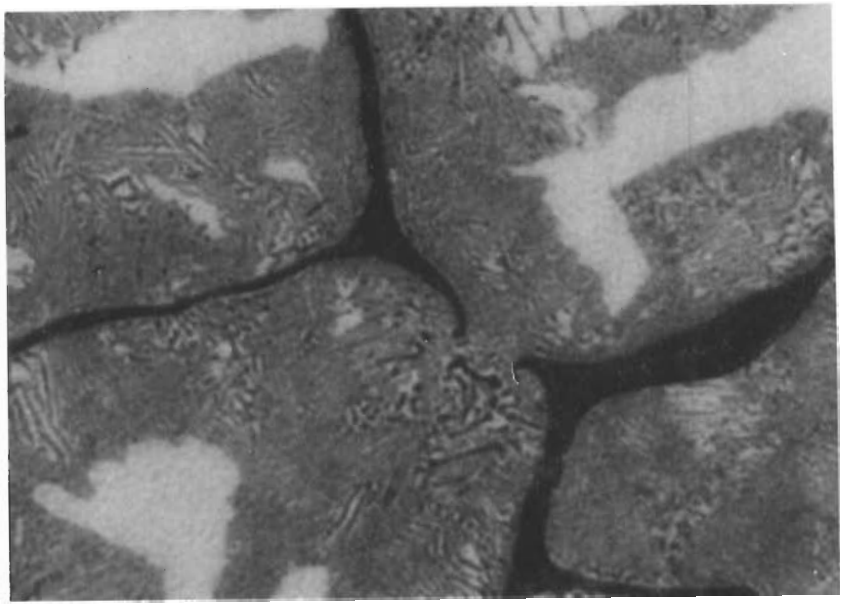

Figure 15. Ta-Mo-C (38-32-30 At%), Equilibrated at 2450°C and Cooled at 4°C per Second. X2500

Lamellar-Type Decomposition Structure of the Subcarbide Phase. Note Progress of the Reaction from the Excess Grain Boundary Metal (Dark Phase) Towards the Grain Centers, Which Still Contain Some Unconverted Me_2C-Solid Solution.

X-Ray: Monocarbide, Metal, and Subcarbide Phase.

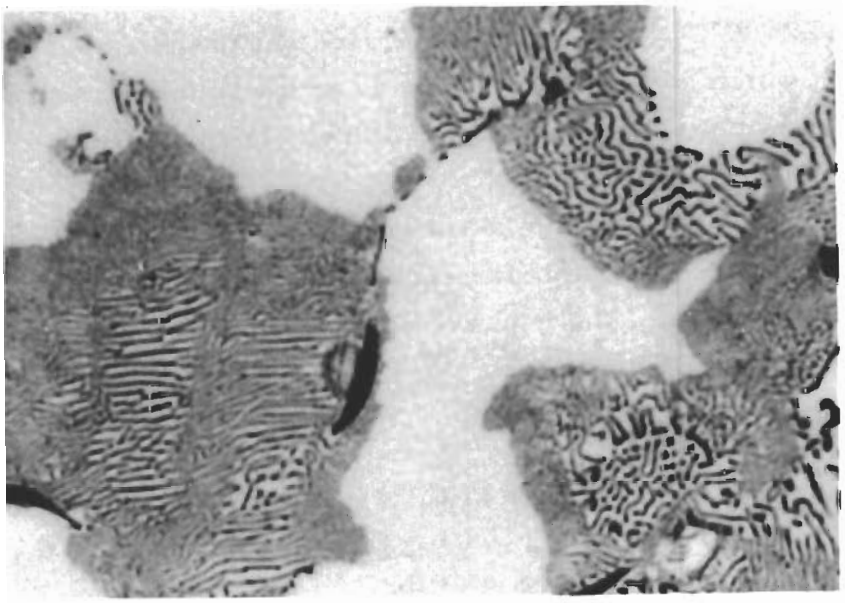

Figure 16. Ta-Mo-C (38-30-32 At%), Equilibrated at 2400°C, and Cooled at 1°C per Second. X2500

Lamellar Structure: Decomposed $(Ta, Mo)_2C$-ss, Consisting of Metal + Monocarbide.

Light Areas: Undecomposed $(Ta, Mo_2C$-ss

From the available information, the decomposition reaction is easily reconstructed: At 2230°C, the two, three-phase equilibria, i.e.

$$(Ta, Mo)\text{-}ss_{(1)} + (Ta, Mo)_2C\text{-}ss_{(1)} + (Ta, Mo)C_{1-x}(B1)\text{-}ss_{(1)}$$

and

$$(Ta, Mo)\text{-}ss_{(2)} + (Ta, Mo)_2C\text{-}ss_{(2)} + (Ta, Mo)C_{1-x}(B1)\text{-}ss_{(2)}$$

which terminate both subcarbide phases at lower temperatures, merge into a single tie line. At the critical point, the decomposition reaction can be written as:

$$(Ta, Mo)_2C \longrightarrow (Ta, Mo) + (Ta, Mo)C_{1-x} ,$$

and thus corresponds to the binary eutectoid reaction.

The ζ-phase was not found in samples equilibrated at 2200°C and 2500°C. Experiments carried out in the range of 1900-2100°C on samples which contained the ζ-phase at lower temperatures showed that this phase was not present at temperatures above 2050°C.

If we take into account the equilibria involving the ζ-phase at somewhat lower temperatures, the most plausible process leading to the disappearance of the ζ-phase corresponds to a Class III, ternary peritectoid reaction according to:

$$\zeta \xrightarrow{T \geq 2050°C} (Ta, Mo) + (Ta, Mo)_2C + (Ta, Mo)C_{1-x}$$

In the experimental isotherm at 2500°C (Figure 17), the molybdenum-rich alloys located between the metal and subcarbide solid solutions are already partially molten. Although less pronounced than in the isotherms at 1500°, 1800°, and 2200°C, the tie lines in the two-phase fields: metal + subcarbide and metal + monocarbide are still strongly inclined towards the tantalum-rich carbide compositions.

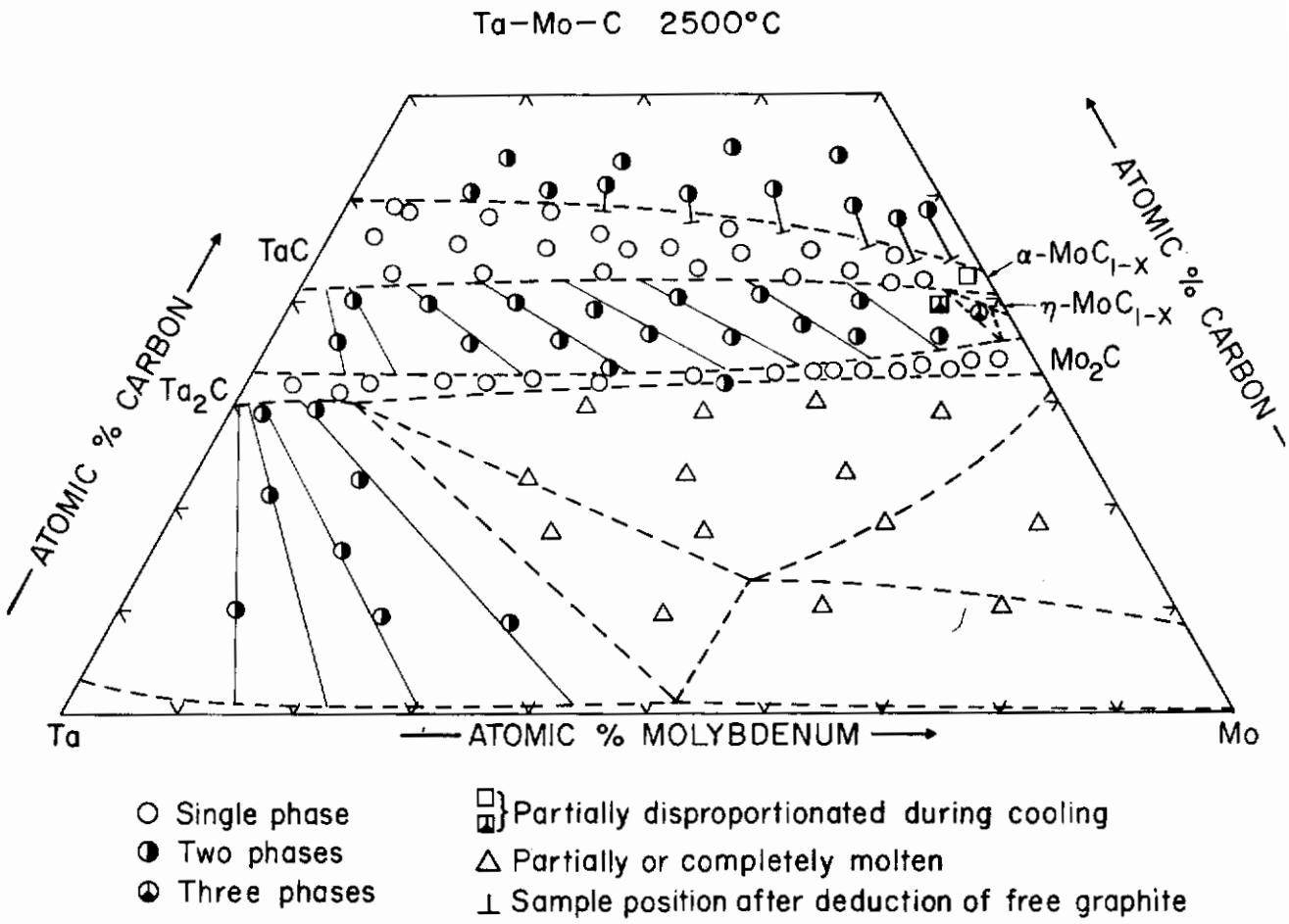

Figure 17. Location and Qualitative Phase Evaluation of the Alloys Equilibrated at 2500°C.

The solidus temperatures along the metal + subcarbide eutectic trough vary smoothly between the eutectic temperatures of the binary metal-carbon systems (Figure 18). Although the microstructures of melted alloys located near the boundary systems closely resemble the structures of the binary Me + Me_2C eutectics (Figures 19 and 20), the bivariant eutectic crystallization in the ternary becomes clearly evident in alloys containing approximately equal amounts of tantalum and molybdenum (Figure 21).

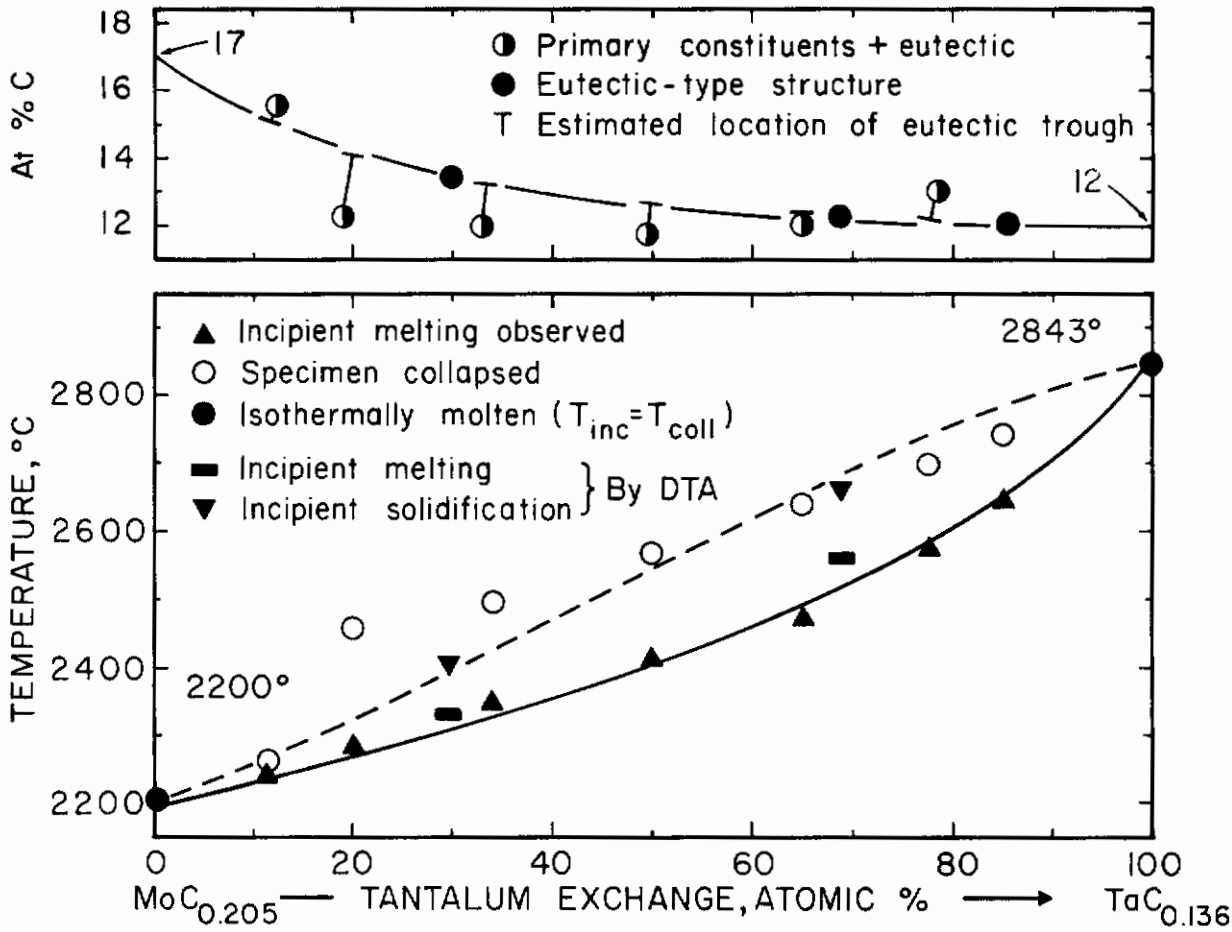

Figure 18. Melting (Bottom) and Microscopic Evaluation (Top) of Alloys Located Along (Ta, Mo)+$(Ta, Mo)_2C$ Eutectic Trough.

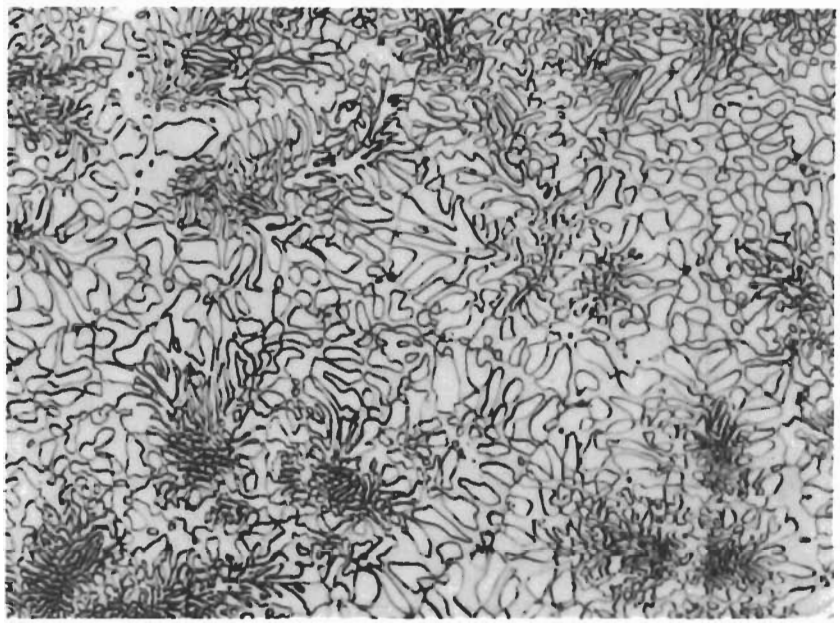

Figure 19. Ta-Mo-C (10-75-15 At.%), Rapidly Cooled from 2300°C. X475

Eutectic-Like Structure Near the Molybdenum-Carbon Binary.

Figure 20. Ta-Mo-C (75-13-12), Rapidly Cooled from 2800°C. X1000

Eutectic-Like Structure Near the Tantalum-Carbon Binary.

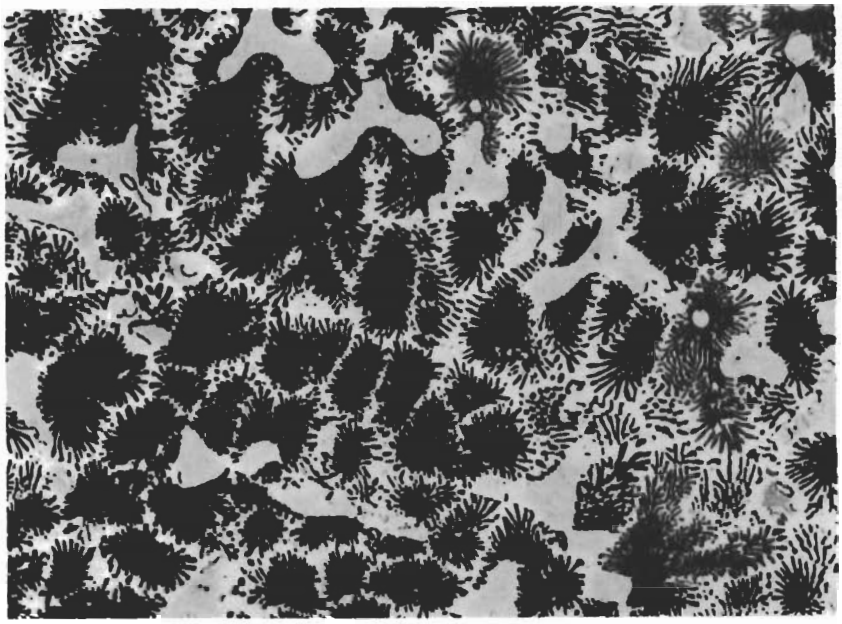

Figure 21. Ta-Mo-C (43-45-12 At%) Melted and Rapidly Cooled X475
Primary Crystallized Metal Solution in a Matrix of Bivariantly Solidified (Ta, Mo) + $(Ta, Mo)_2C$ Eutectic.

Over a large range of metal compositions, melting of the subcarbide solid solution occurs under decomposition, and only subcarbide alloys located near the molybdenum-carbon binary melted according to the maximum-type (Figure 11). Although both reactions are bivariant in the ternary, a distinction between both types can be accomplished without difficulty by metallographic means as well as by X-rays, since only the peritectic-type of melting will produce other phases as initial products of crystallization and thus exhibit a peritectic-like structure (Figure 22). Non-equilibrium crystallization of alloys which melt according to the maximum-type will result only in coring. Based on the microscopic examination of approximately 15 alloys, the transition from maximum to peritectic-type melting in the subcarbide occurs at a tantalum exchange of 10 ± 2 At%. The respective composition itself is characterized by a congruent melting point.

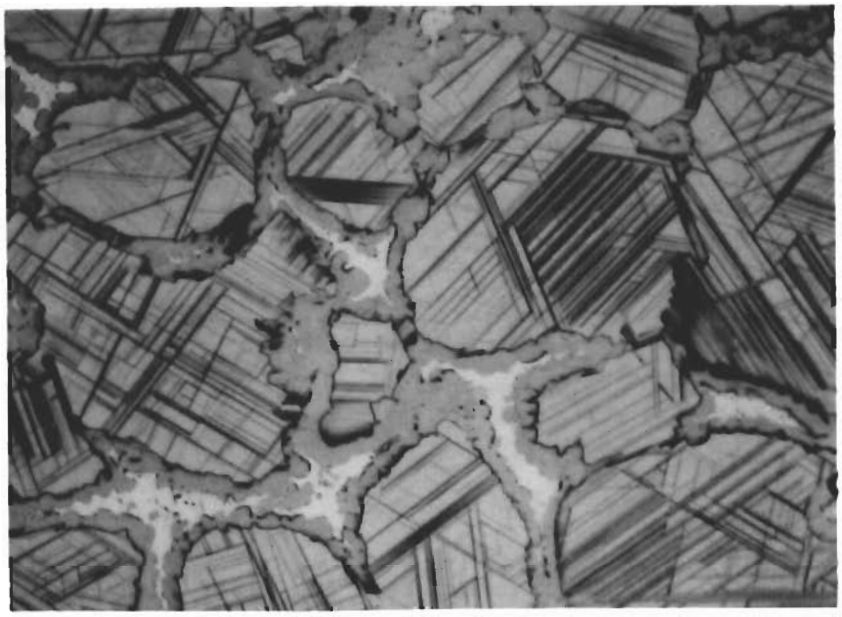

Figure 22. Ta-Mo-C (52-15-33 At%), Rapidly Cooled from 3300°C. X700

Peritectic-Like Structure Consisting of Primary Crystallized Monocarbide (with Localized Subcarbide Precipitations), Secondary Crystallized Subcarbide (Surrounding the Monocarbide Phase) and Rest-Eutectic.

The solidus temperatures of the monocarbide solid solution are a function of the relative metal content as well as the carbon concentration. In order to locate the concentration line of the maximum solidus, it was necessary to examine the entire solidus envelope of the solid solution. For the particular case of the $(Ta,Mo)C_{1-x}$-phase, this task proved fairly difficult, because the large melting point differences between the binary carbides caused the ternary alloys to melt extremely heterogeneously. The problem of detecting incipient melting was finally overcome by using the temperature detection system of the derivative thermal analysis apparatus as a sensor for the phase change, while the temperatures were measured independently with an optical pyrometer. In this manner, the datum points shown in Figure 23 were extracted from measurements on approximately 60 monocarbide alloys and are judged to be representative of the maximum solidus temperatures of the monocarbide phase. As expected from the melting behavior, all monocarbide alloys were heavily cored when quenched from near liquidus temperatures (Figure 24), and the X-ray patterns were diffuse.

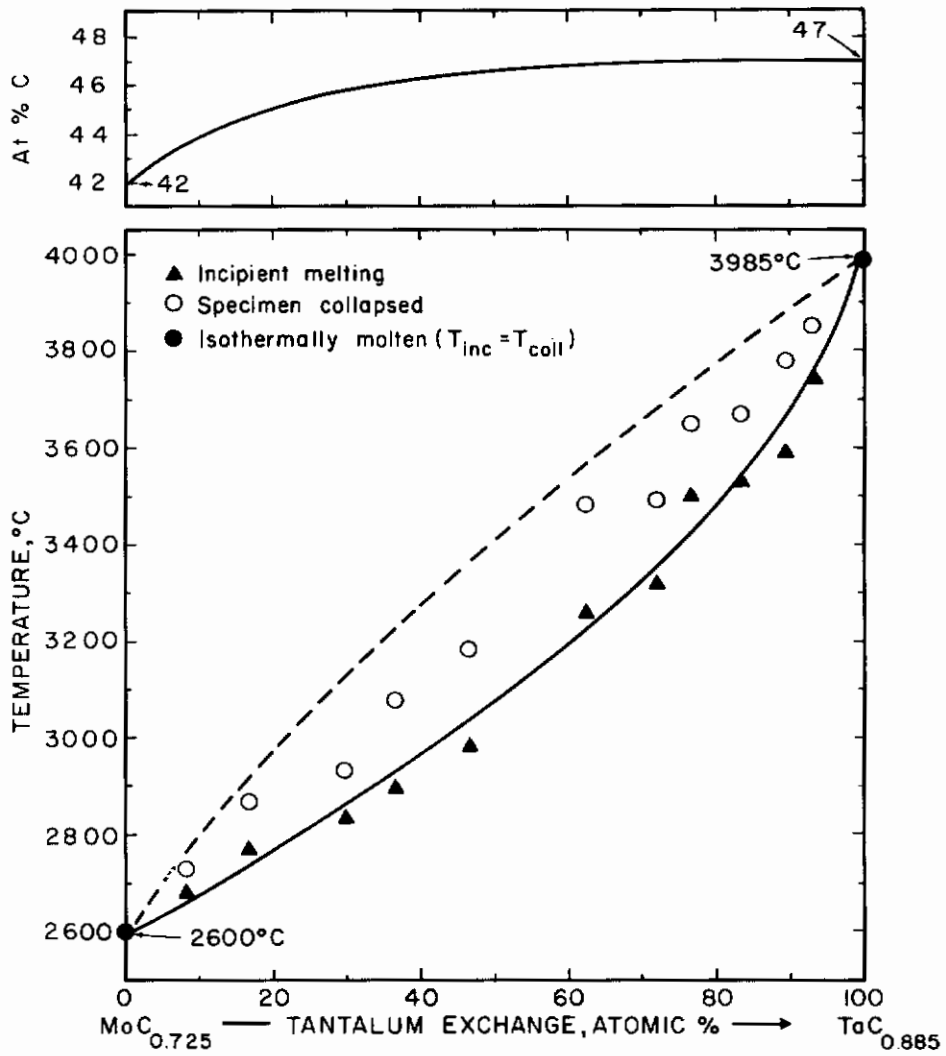

Figure 23. Maximum Solidus Temperatures for the Tantalum-Molybdenum Monocarbide Solid Solution.

Top: Concentration Line of the Maximum Solidus.

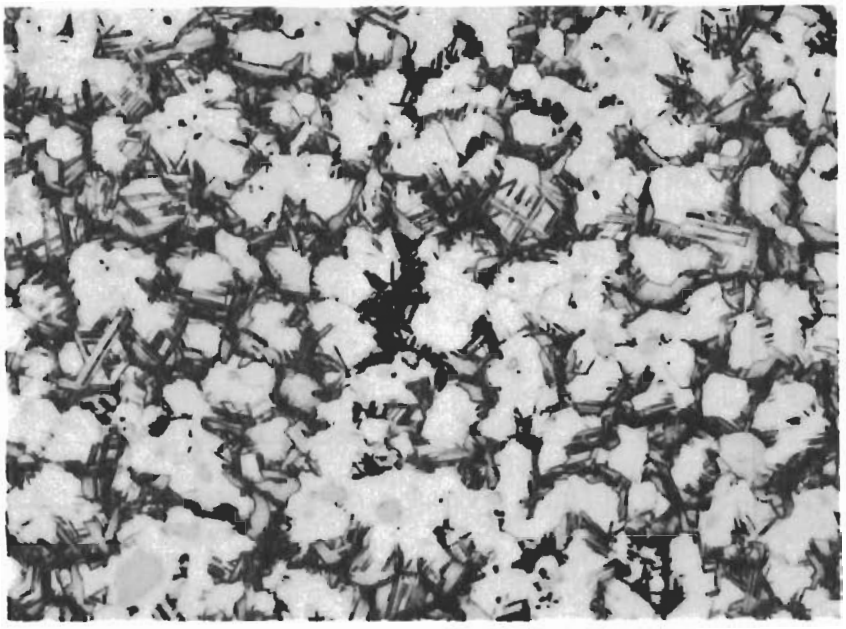

Figure 24. Ta-Mo-C (5-52-43 At%), Rapidly Cooled from 2730°C. X325

Cored Monocarbide Solid Solution. Note the Decomposition of the Mo-Rich Monocarbide Phase, which Solidified Last, Whereas the First Crystallized, Ta-Richer Solution, Remained Single-Phased.

The metal- and carbon-rich boundaries of the monocarbide phase at solidus temperatures were located mainly by metallographic inspection of quenched alloys, since rapid precipitation of metal or subcarbide phase from the tantalum-rich monocarbide prevented the retention of the high temperature equilibrium; in excess graphite-containing alloys, the low scattering power of carbon did not permit detection of this free graphite by X-rays.

In the composition area: monocarbide + graphite, the solidus temperatures along the eutectic trough vary smoothly between the binary eutectics (Figure 25). Melting across the entire concentration range was extremely heterogeneous, making the location of the eutectic trough by microscopic analysis rather difficult. A typical microstructure from the monocarbide + graphite region is shown in Figure 26.

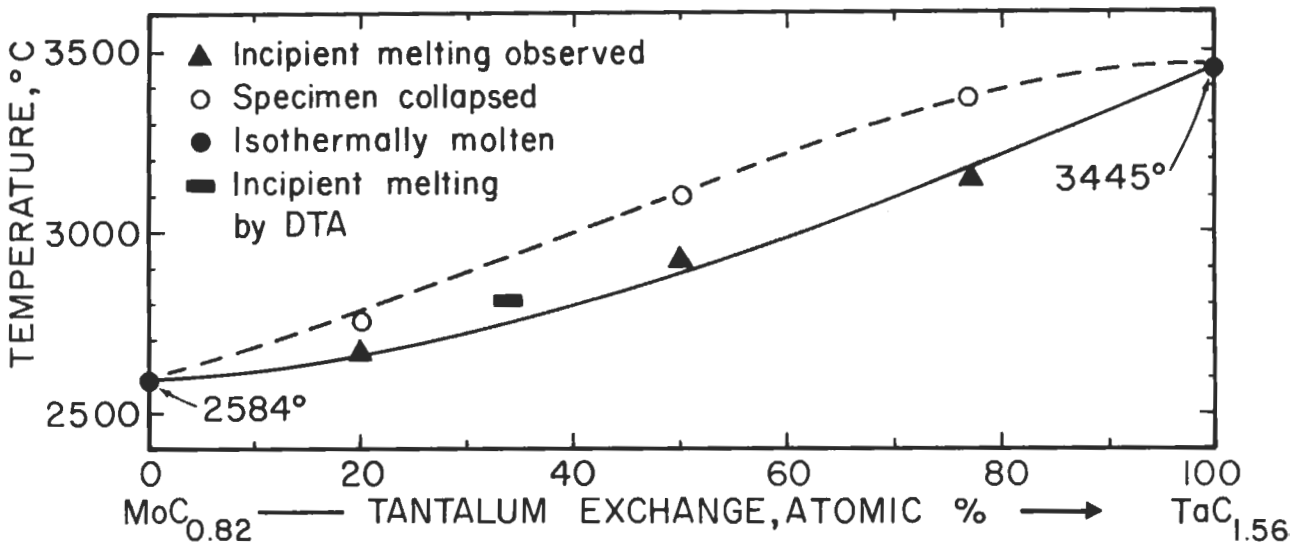

Figure 25. Melting Along the $(Ta,Mo)C_{1-x}$ + C Eutectic Trough

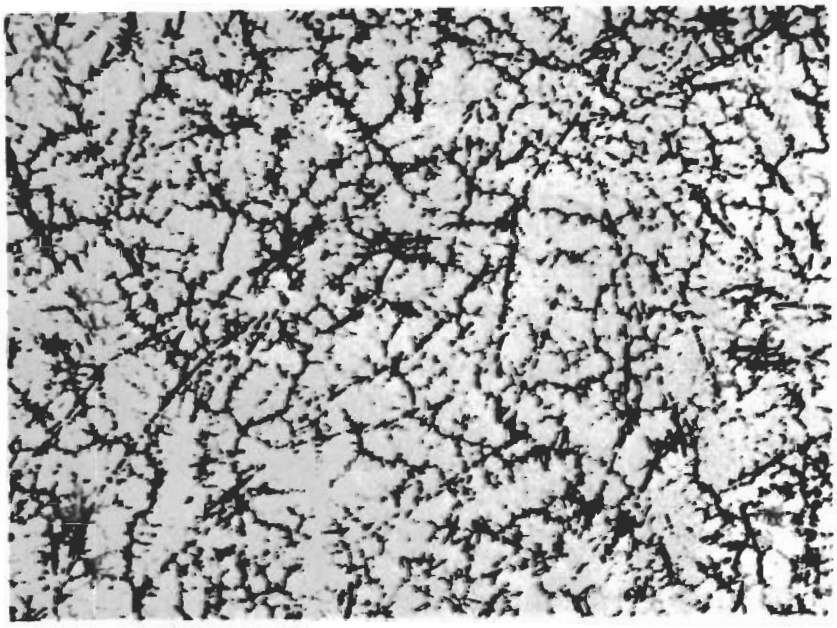

Figure 26. Ta-Mo-C (85-45-47 At%), Rapidly Cooled from 2750°C X800

Primary Crystallized Monocarbide and Excess Graphite Formed by Co-Crystallization with the Monocarbide Along the Monocarbide + Graphite Eutectic Trough.

IV. ASSEMBLY OF THE PHASE DIAGRAM

The experimental data have been combined to construct an equilibrium diagram for the Ta-Mo-C system from 1500°C through the melting range. The isometric view of the phase diagram, Figure 27, is supplemented by the flow diagram of the binary and ternary isothermal reactions, Figure 28; two isopleths, Figures 29 and 30, depict more clearly the most important reactions in the system. Another diagram, Figure 31, shows the projected liquidus. To facilitate reading of the equilibrium diagram, but especially for a more efficient use of the phase diagram data, a number of isothermal sections was prepared and is presented in Figures 32(a) through 32(h). A code for the phase symbols used in the isotherms may be found in the reaction diagram, Figure 28.

Because some of the reactions indicated in the phase diagram illustrations were not mentioned in the discussion of the experimental data used to arrive at the gross-features of the system, the necessary background information will be given now:

The continuation of the order-disorder transition into the ternary was studied by differential-thermoanalytical techniques on twelve alloys which contained between 30 and 34 At% carbon and between one and fifteen At% molybdenum. In the alloy series at 32 At% C, the transition temperatures decreased smoothly from ~2150°C for the binary carbide to ~2020°C at the phase boundary in the ternary (Figure 11). No signs for a phase discontinuity in the transformation process could be detected by post-experimental, microscopic inspection of these alloys.

A somewhat different behavior was found in the alloy series containing between 32.5 and 33 At% C: Originating at 2170°C in the binary, the transition temperatures drop to approximately 2080°C at a molybdenum exchange near 8 At%; in the DTA-thermograms of the same alloys, a second, barely discernible reaction was indicated to proceed at ~1980°C. Alloys containing more than ~8At% Mo showed the same transition temperatures measured in the alloy series at 32 At% C at comparable molybdenum contents. Finally,

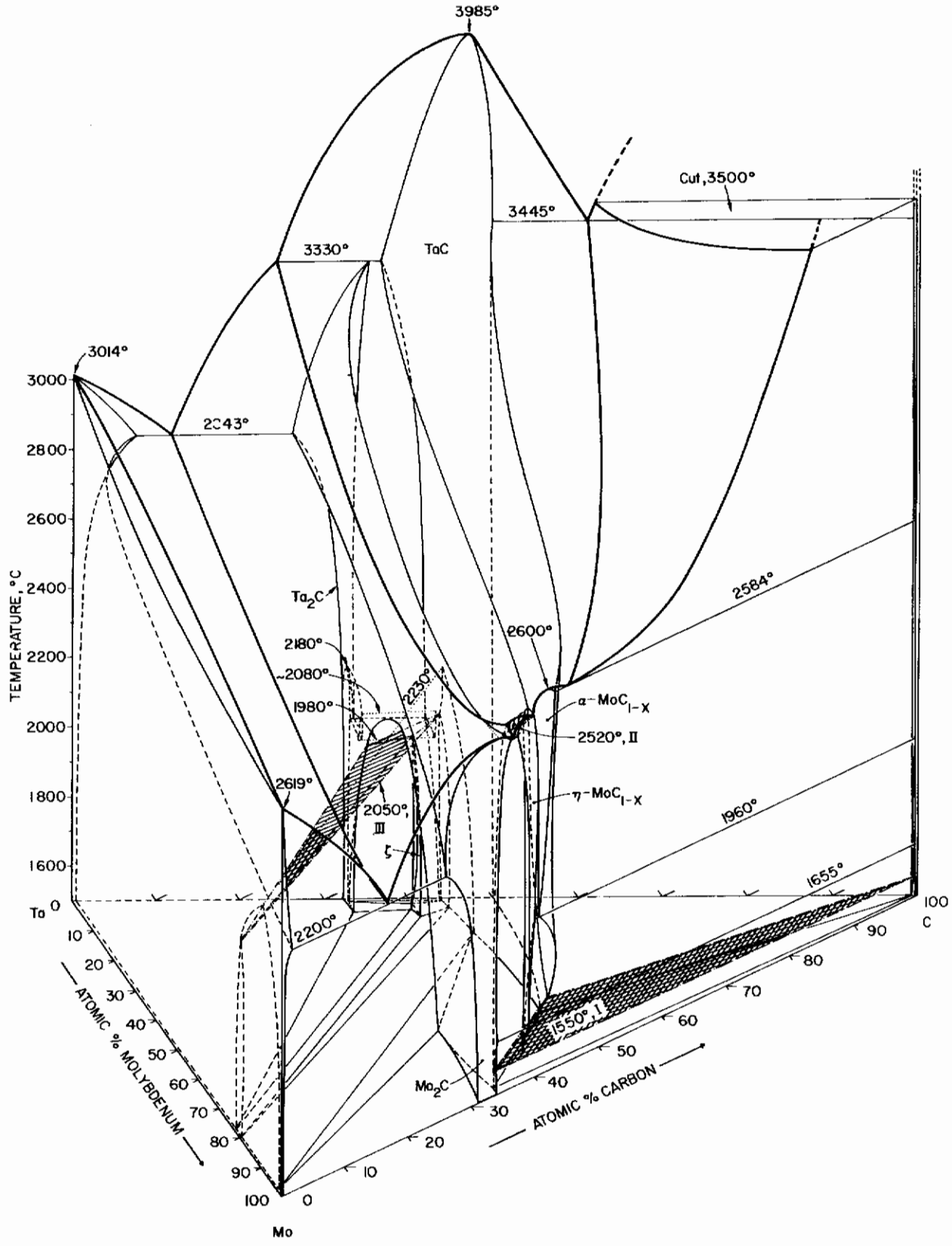

Figure 27. Constitution Diagram for the System Ta-Mo-C.

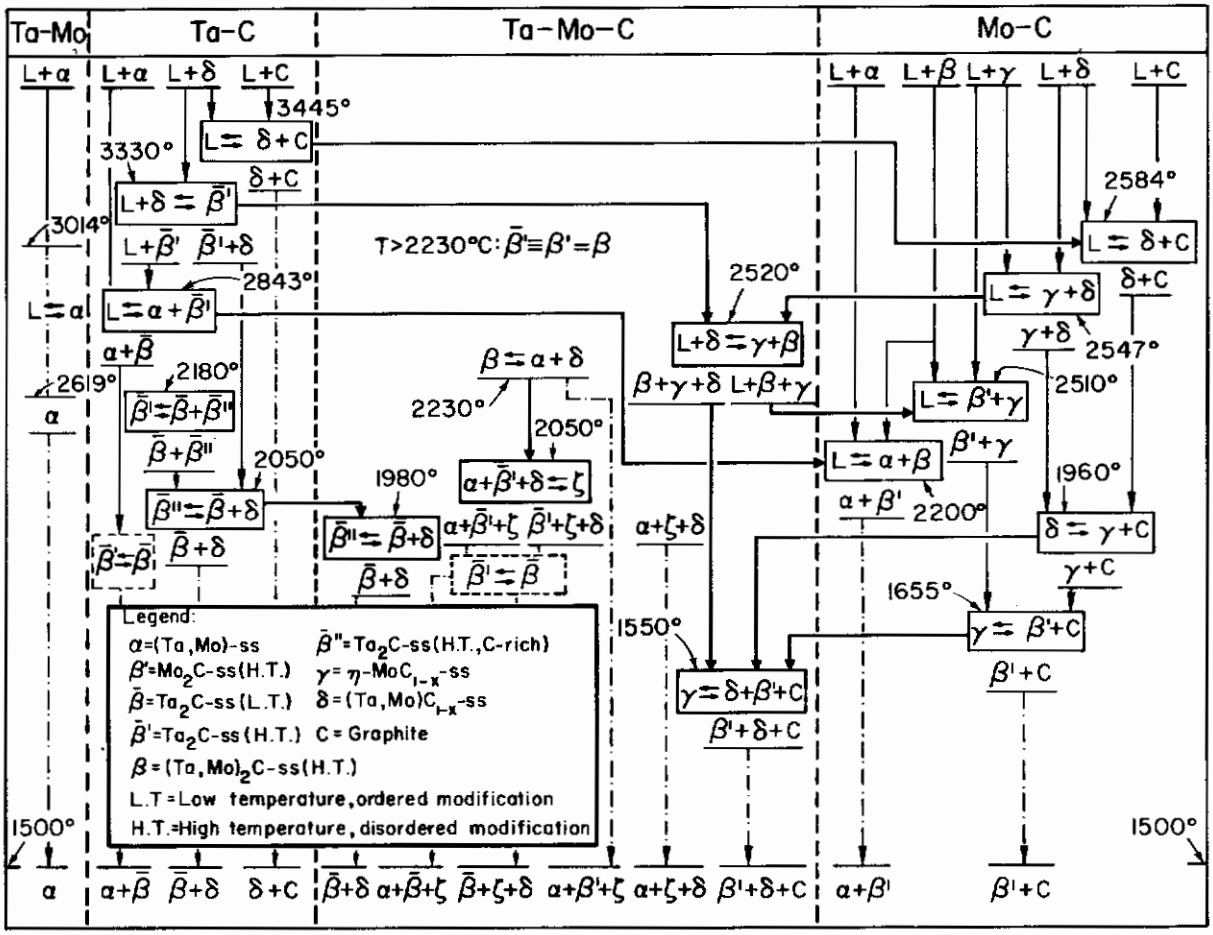

Figure 28. Scheil-Schulz Reaction Diagram for Ternary Ta-Mo-C Alloys.

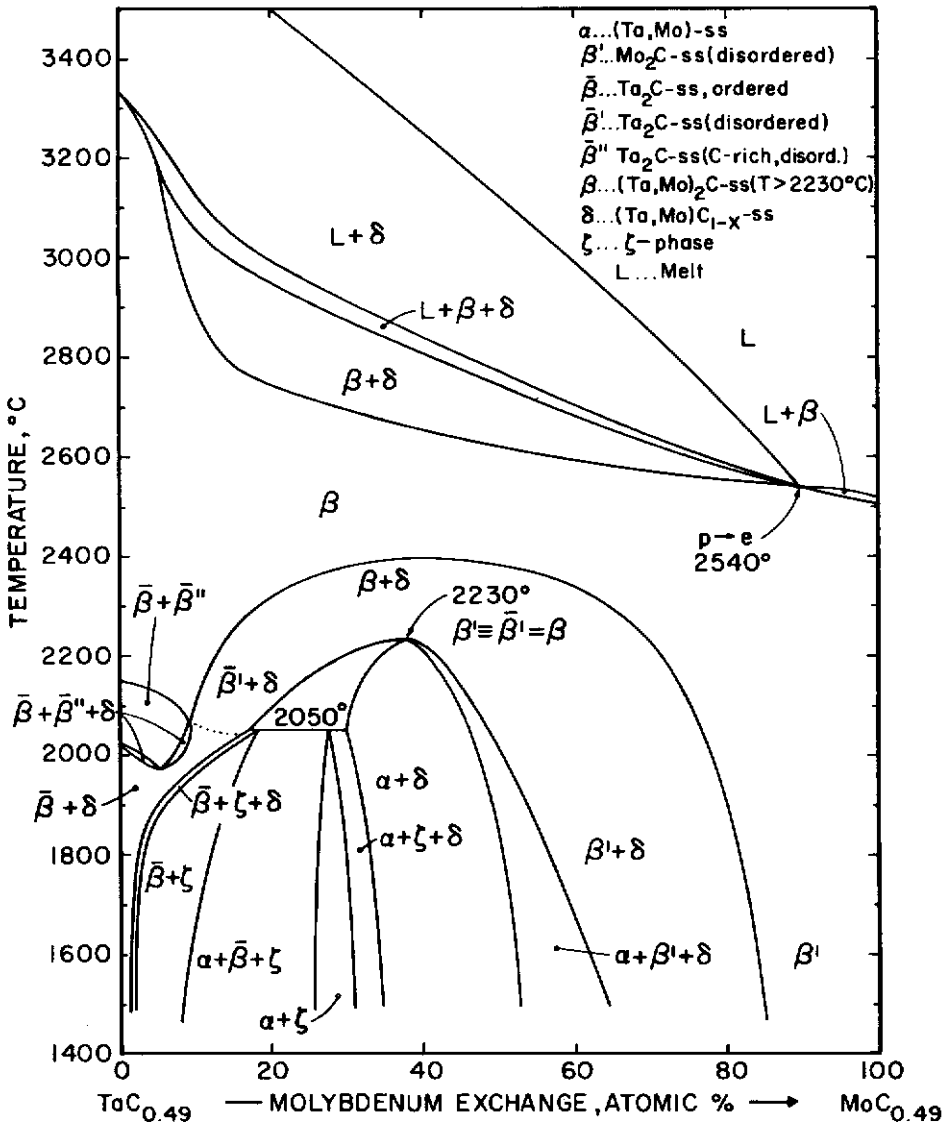

Figure 29. Isopleth Along $TaC_{0.49}$-$MoC_{0.49}$

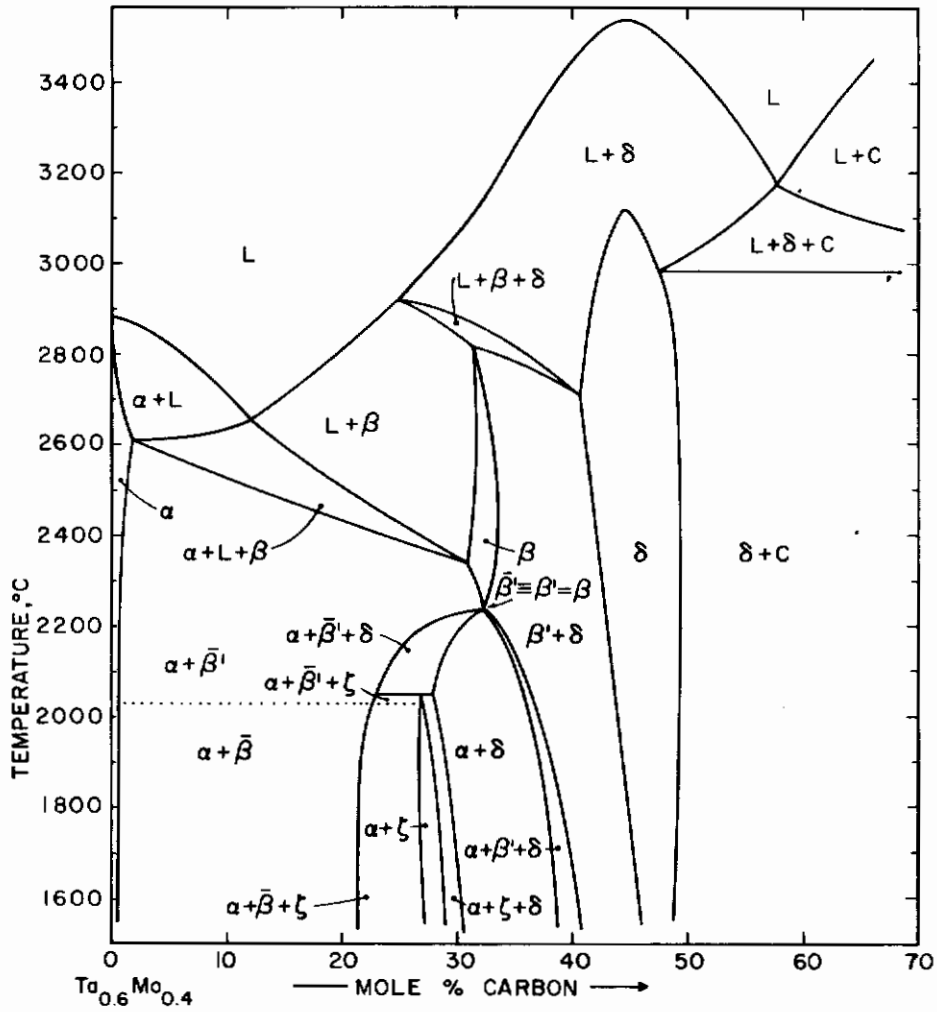

Figure 30. Isopleth Along $(Ta_{0.6}Mo_{0.4})$-C .

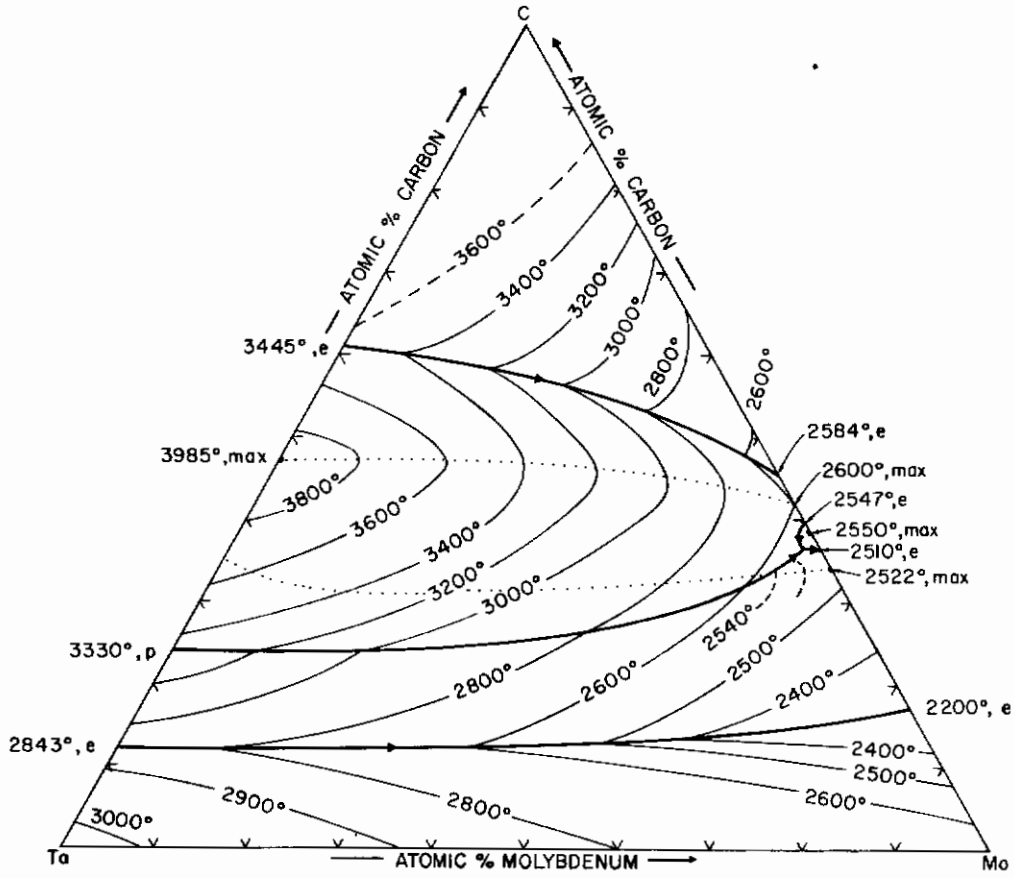

Figure 31. Liquidus Projections for the Ta-Mo-C System, Partially Estimated.

(Dotted Curves Indicate Concentration Lines of the Maximum Solidus of the Subcarbide and the Monocarbide Solid Solution).

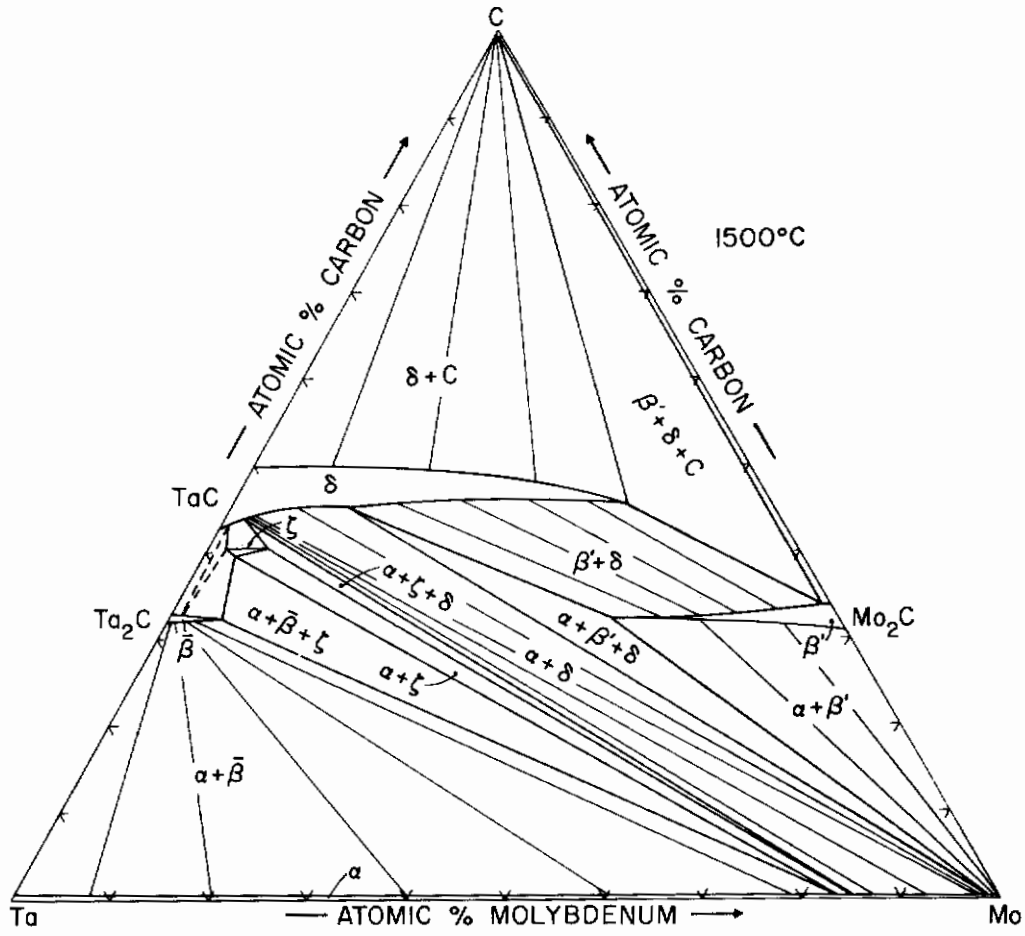

Figure 32 (a).

Figures 32(a) through 32(h):

Isothermal Sections for the Ta-Mo-C System.

(a) 1500°C	(e) 2500°C
(b) 1800°C	(f) 2800°C
(c) 2050°C	(g) 3000°C
(d) 2230°C	(h) 3500°C

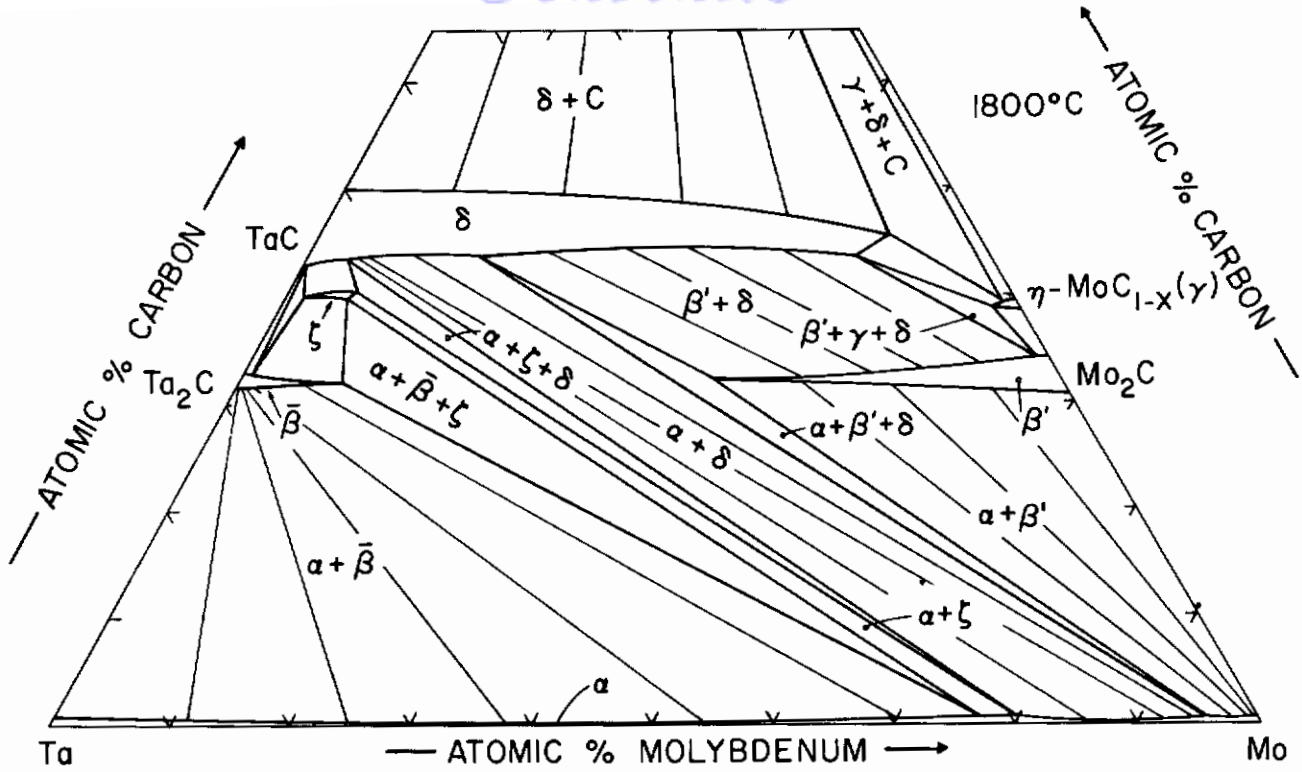

Figure 32(b).

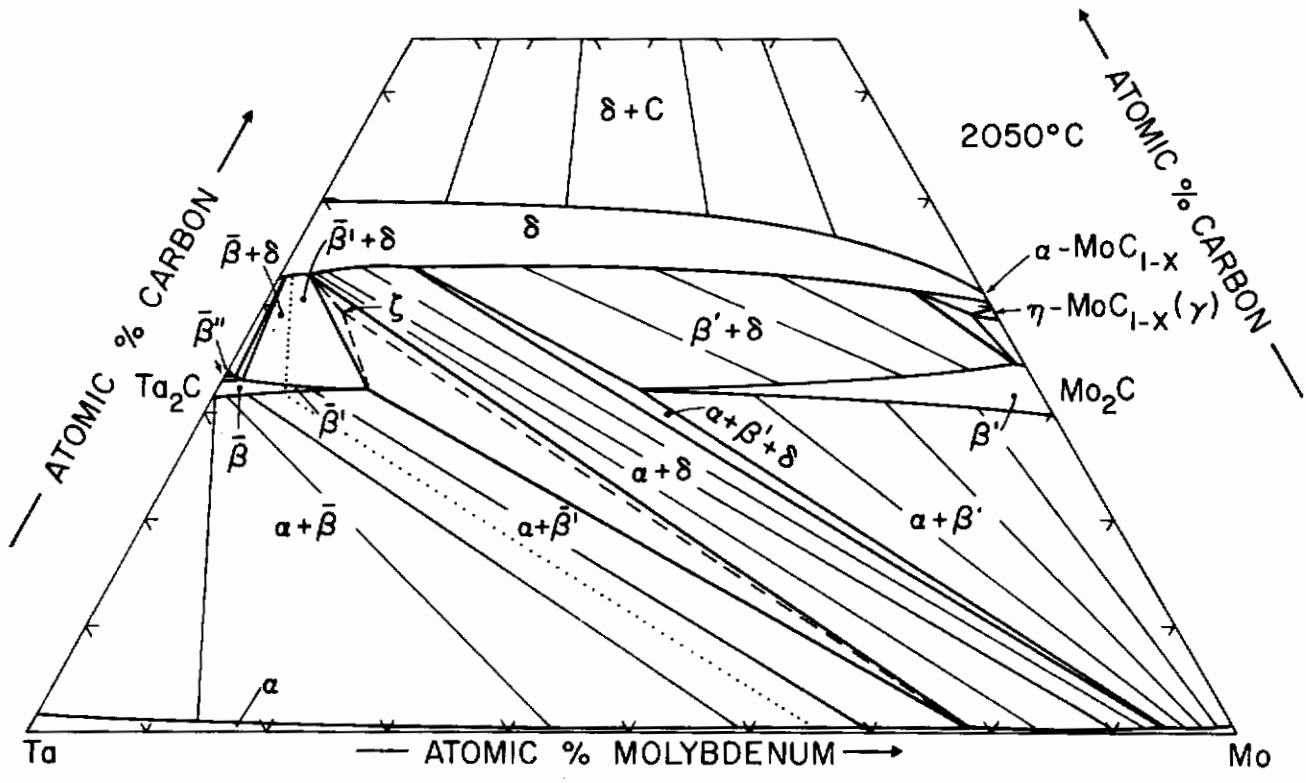

Figure 32(c).

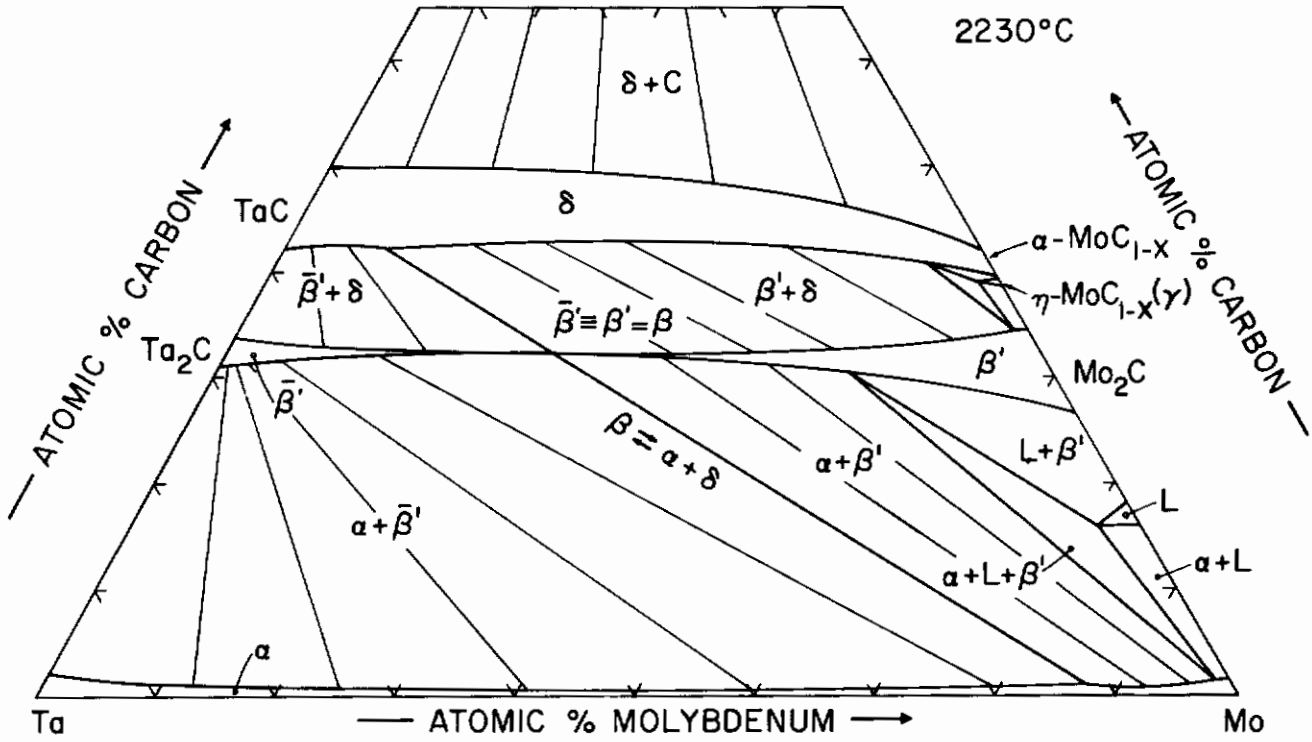

Figure 32(d).

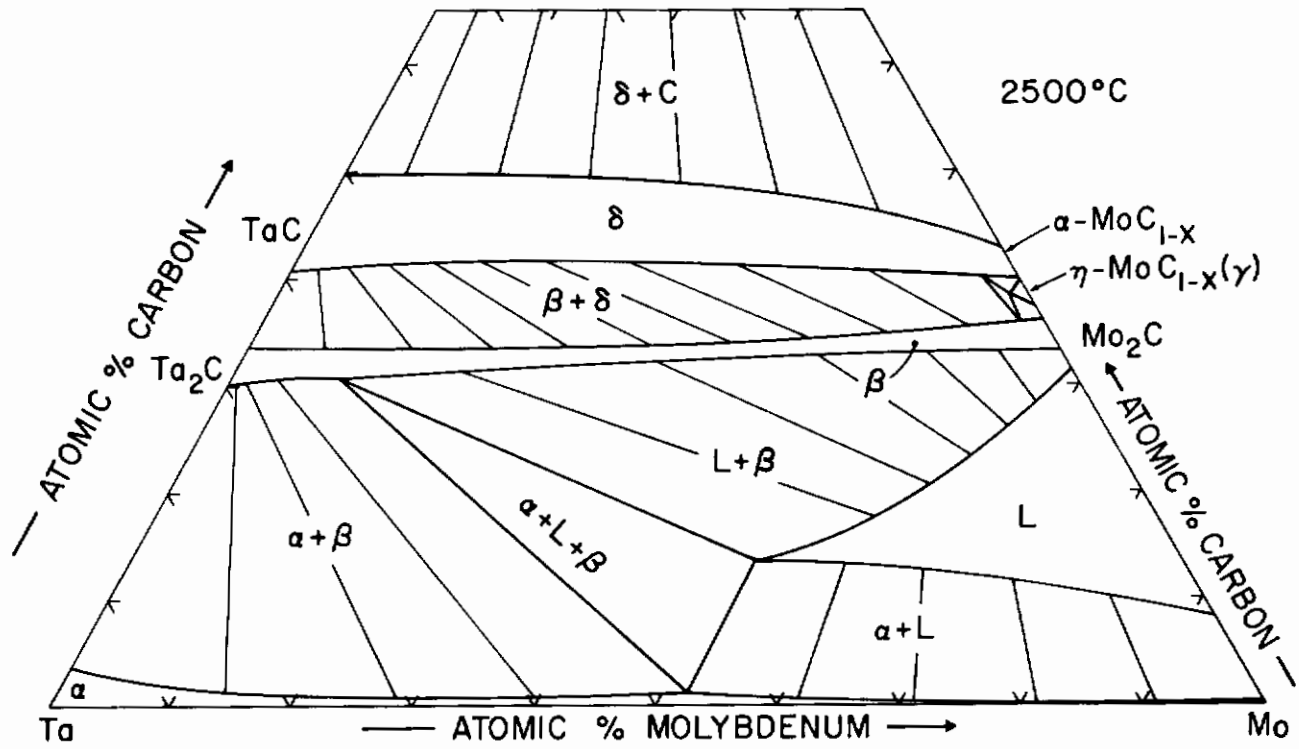

Figure 32(e).

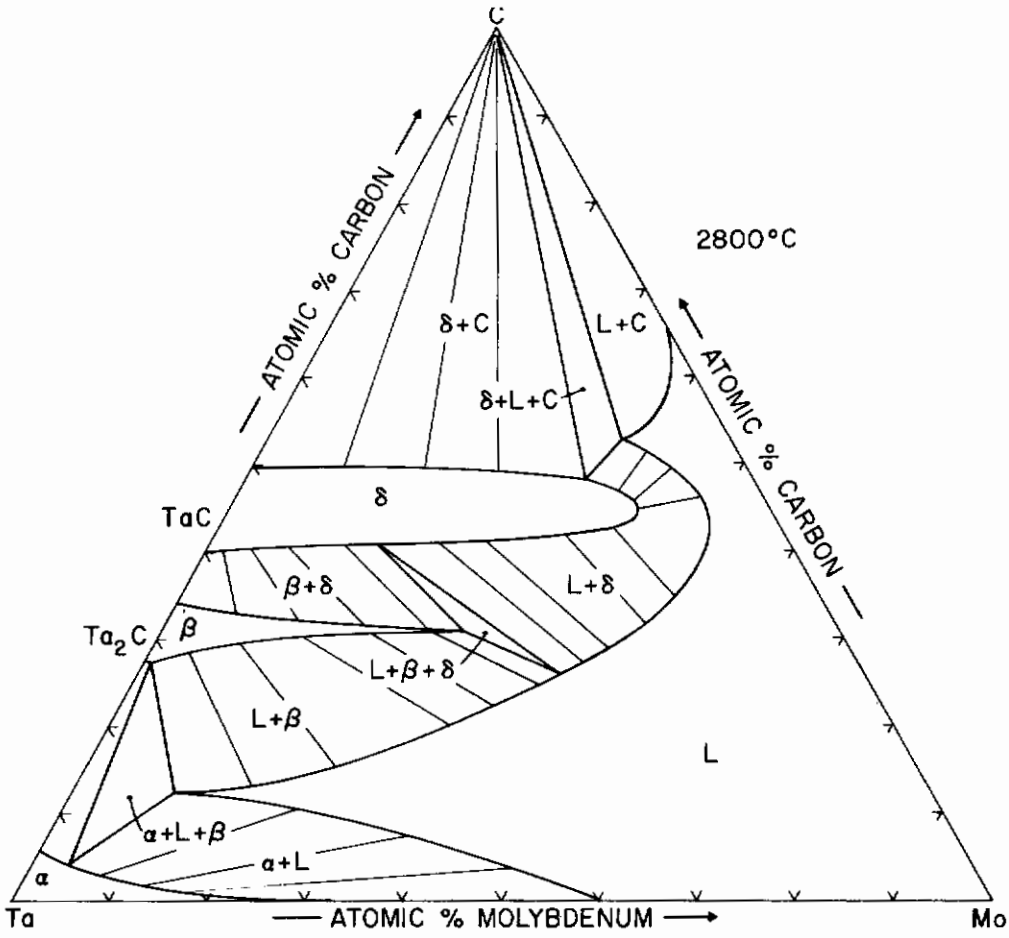

Figure 32(f).

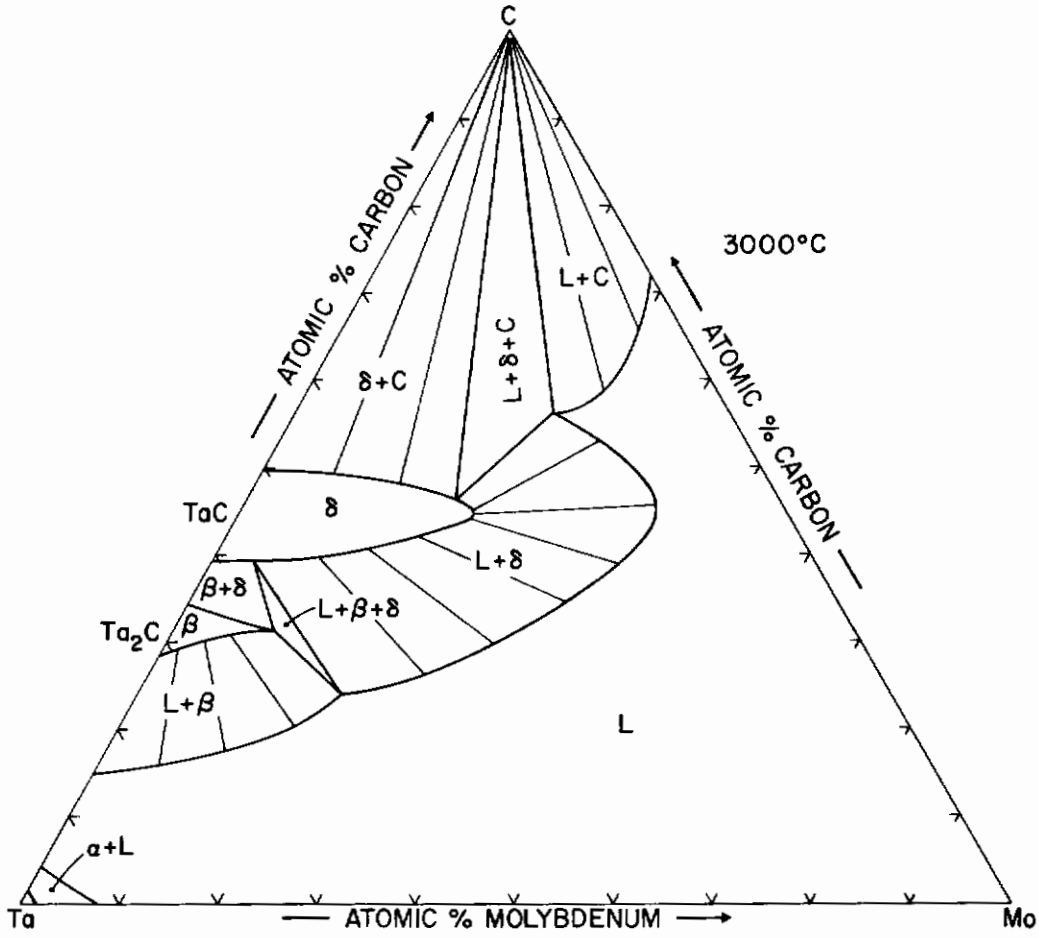

Figure 32(g).

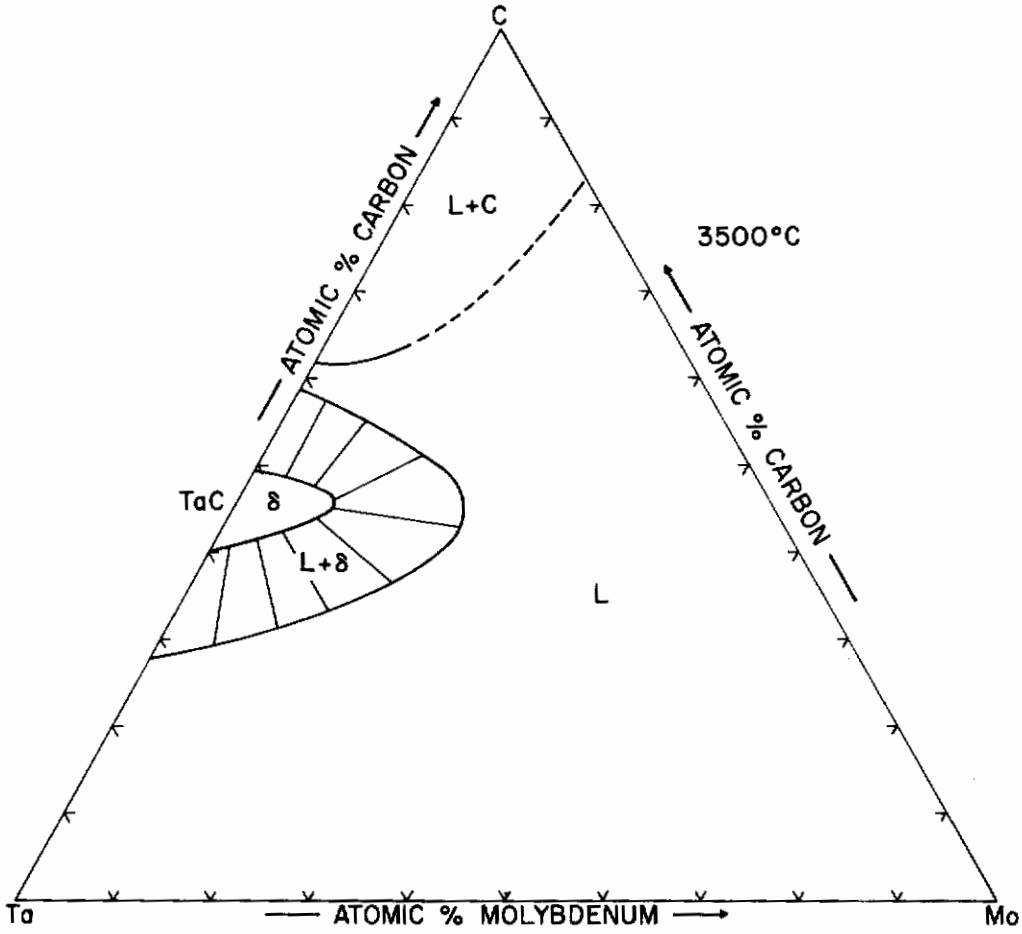

Figure 32(h).

in the alloy series at 34 At% C, the thermal arrests first showed a slight drop from 2020°C in the binary to approximately 1980°C at 8 At% Mo, and then increased slightly to approximately 2050°C as the terminal solid solution was approached.

From the available information supplemented by microscopic data, the following sequence of reactions was found to be compatible with the experimental results and was adopted for the description of the phase equilibria within this concentration region:

In the substoichiometric (< 32 At%) Ta_2C-solid solution, the transition continues as a single-phased, second order transition into the ternary. In alloys containing between 32.5 and 33 At% C, the temperatures of the phase separation into ordered and disordered phase, is lowered by molybdenum additions. With increasing molybdenum content, the carbon-rich boundary of the subcarbide phase retracts to substoichiometric compositions, and the phase separation finally ceases to exist. This behavior agrees with the observation that the phase separation never was detected in the substoichiometric binary carbides[8, 22]. The disordered modification, which is terminated in a eutectoid reaction at 2020°C in the binary Ta-C system, is stabilized to lower temperatures by molybdenum additions. At temperatures near 1980°C, the two, three-phase equilibria, viz.

$$Ta_2C\text{-ss, ordered}(\bar{\beta})_{(1)} + Ta_2C\text{-ss, disordered, C-rich}(\bar{\gamma}'')_{(1)} + TaC\text{-ss}(\delta)_{(1)} \quad (1)$$

and

$$TaC\text{-ss, ordered}(\bar{\beta})_{(2)} + Ta_2C\text{-ss, disordered, C-rich}(\bar{\gamma}'')_{(2)} + TaC\text{-ss}(\delta)_{(2)} \quad (2)$$

of which the first originates at the eutectoid reaction isotherm at 2020°C in the binary Ta-C system, and the second at the critical tie line at 2080°C, merge into a single tie line. The resulting equilibrium type corresponds to the binary eutectoid, and the overall reaction proceeding at this temperature can be written as:

$$Ta_2C\text{-ss, disordered, C-rich } (\bar{\gamma}'') \xrightarrow{T \leq 1980°C} Ta_2C\text{-ss, ordered } (\bar{\gamma}) + TaC\text{-ss}$$

The occurrence of the Class II ternary isothermal reaction at 2520°C was deduced from X-ray and metallographic analysis of melted ternary alloys. The ternary range of homogeneity of η-MoC_{1-x} is limited to tantalum concentrations below 4 At%. Towards lower temperatures, the phase is terminated in a Class I, eutectoid reaction approximately 100°C lower than that of the binary alloy. Substitution of small quantities of tantalum into the η-MoC_{1-x}-lattice significantly reduces the rate of decomposition, and cooling rates of less than 0.5°C per second were necessary in the DTA-runs to detect the decomposition reactions.

The temperature of the phase separation in Mo_2C is also lowered in the ternary, as verified by differential-thermoanalytical studies (Figures 11 and 33). However, contrary to the behavior of the Ta_2C-rich alloys, the decomposition temperature of the carbon-rich, disordered Mo_2C-phase, is raised in the ternary.

The phase separation, recognized by its characteristic, intragranular veining structure, Figures 34(a) and 34(b), persists to a tantalum exchange of approximately 9 At%, after which the reaction appears to proceed single-phased. Two isothermal, ternary reactions are expected to result from the order-disorder transition in the Mo_2C solid solution:

First, the terminating point of the phase separation at ~1400°C and ~9 Mole% Ta_2C is characterized by a limiting tie line which then expands to a three-phase equilibrium:

$$(Mo, Ta)_2C\text{-ss, disordered, C-rich} + (Mo, Ta)_2C\text{-ss, ordered} + (Ta, Mo)C_{1-x}\text{-ss}$$

towards lower temperatures. This three-phase equilibrium interacts at ~1200°C with another three-phase equilibrium,

$$(Ta, Mo)C_{1-x}\text{-ss} + (Mo, Ta)_2C\text{-ss, ordered} + \text{Carbon}$$

in a Class II ternary reaction according to:

$$(Ta, Mo)C_{1-x}\text{-ss} + (Mo, Ta)_2C\text{-ss, disordered, C-rich} \xrightarrow{T \leq 1200°C} (Mo, Ta)_2C\text{-ss, ordered} + C$$

and finally terminates at 1190°C at the eutectoid point in the Mo-C binary.

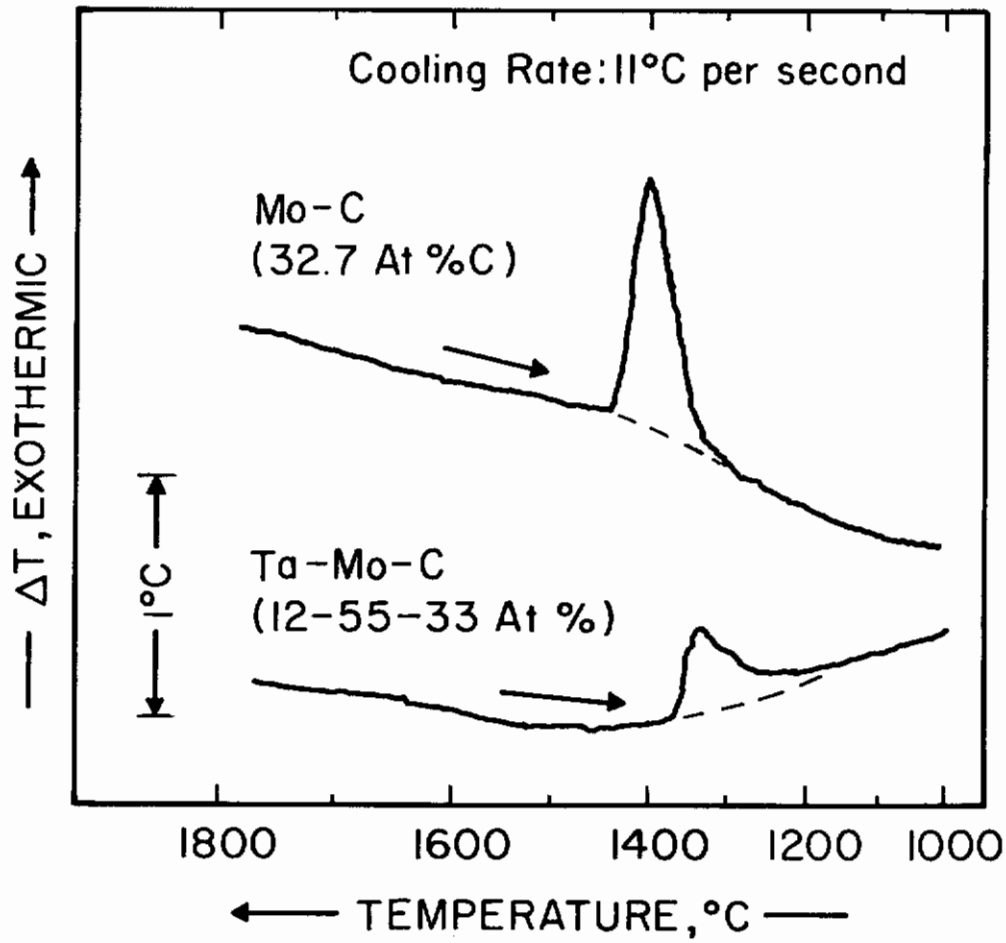

Figure 33. Sublattice Order-Disorder Transformation in the Binary Mo_2C Phase (Top) and a Ternary $(Ta, Mo)_2C$ Alloy.

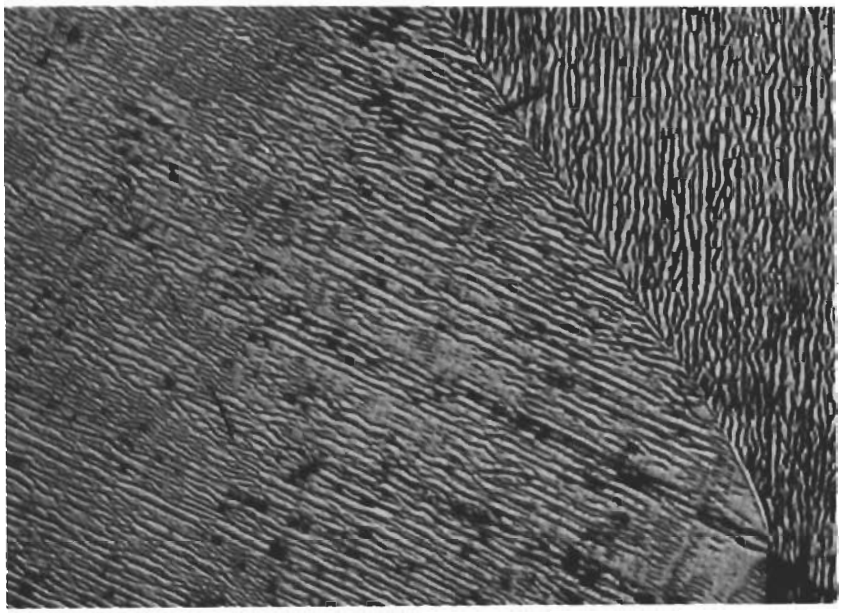

Figure 34(a) Mo-C (32.0 At% C), Cooled at 10°C per Second from 1700°C. X1000

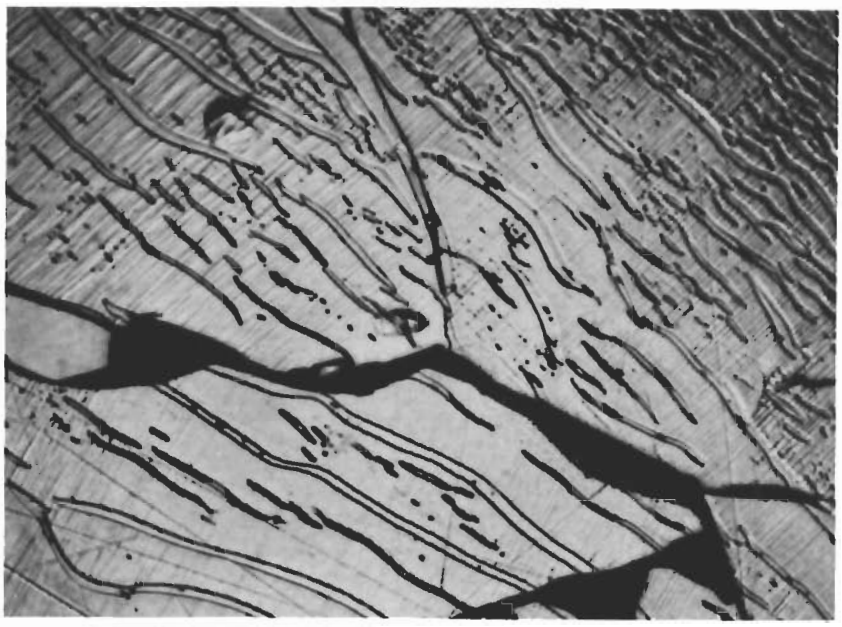

Figure 34(b). Ta-Mo-C (5-62-33 At%), Cooled at 6°C per Second from 1500°C. X625

Figures 34(a) and 34(b):

Subgrain Disproportionation into Ordered and Disordered Phases of Mo_2C (34a) and a Ternary (Ta, Mo)C Solid Solution (34b).

At temperatures slightly above 1400°C, the two-phase range

$$(Mo, Ta)_2C\text{-ss, disordered, C-rich} + (Mo,Ta)_2C\text{-ss, ordered}$$

forms a wedge in the subcarbide solid solution. This wedge gradually narrows with increasing temperature and finally closes at 1430°C in the Mo-C binary. Above this temperature, the molybdenum-rich solid solution now contains only the disordered phase.

V. DISCUSSION

The most significant feature in the lower temperature ternary phase equilibria, no doubt, concerns the interruption of the subcarbide solid solution by a two-phase equilibrium between the monocarbide and the metal phase.

From a crystallographic point of view, this fact appears, at least at the first glance, rather surprising, since, from size considerations, the subcarbides should be miscible. But even discounting these expectations, and taking into account the possible formation of a miscibility gap due to differences in the ordered structures, the problem of an explanation for this interruption is not greatly changed, because one would then expect the formation of an equilibrium between both terminal subcarbide solid solutions.

In order to arrive at a possible explanation for these phase phenomena, it is necessary to compare the concentration-dependent thermodynamic stability of ternary subcarbides with those of coexisting mixtures of monocarbide and metal solid solutions.

Since the homogeneity ranges of the subcarbides are fairly small in respect to graphite in the temperature range of interest, and the low carbon boundary of the monocarbide solid solution is nearly parallel to the Ta-Mo binary; the simplified thermodynamic approach developed earlier[23] is adequate for a description of the ternary equilibria. Another reason for choosing the simplified method concerns the fact that the exact variation of the free

energies across the homogeneity ranges of the carbide phases is unknown, and consideration of the general case would have to, therefore, rely on a data fit to the experiment.

Under the assumption of the simplified treatment, namely that the free energy of the phase solutions is allowed to vary only with the metal exchange, the conditional equation for the tie line distribution in any two phase field $(A, {}_{x'_A}, B_{x'_B})C_u + (A_{x''_A}, B_{x''_B})C_v$ is given by[23]:

$$\left[\frac{\delta \Delta G_{f,(A,B)C_u}}{\delta x'}\right]_{T,p} = \left[\frac{\delta \Delta G_{f,(A,B)C_v}}{\delta x''}\right]_{T,p} \qquad (1)$$

$\Delta G_{f,(A,B)C_u}$ and $\Delta G_{f,(A,B)C_v}$ are the free energies of formation of the solid solutions $(A,B)C_u$ and $(A,B)C_v$ respectively, and x' and x'' are the mole fractions of A, or B, in the corresponding sublattices (A, B) in the phase solutions $(A,B)C_u$ and $(A,B)C_v$.

The stability condition for a three-phase equilibrium $(A,B)C_u + (A,B)C_v + (A,B)C_w$ can be written as[23]:

$$(v-w)\,\bar{G}_{A(u)} + (w-u)\,\bar{G}_{A(v)} + (u-v)\,\bar{G}_{A(w)} = 0 \qquad (2a)$$

or, the analogous equation for the component B:

$$(v-w)\,\bar{G}_{B(u)} + (w-u)\,\bar{G}_{B(v)} + (u-v)\,\bar{G}_{B(w)} = 0 \qquad (2b)$$

In these equations, the $\bar{G}_{A(i)}$ and $\bar{G}_{B(i)}$ are the partial molar free enthalpies of the components A and B in the phase solutions i ($i = (A,B)C_{u(v,w)}$). Using the binary phases at the respective concentration of the component C(u, v, w) as the reference state, we may separate the partial free enthalpies into base- and concentration-dependent terms and obtain for the equilibrium case:

$$\Delta G_{Z,AC_v} + \overline{\Delta G}^{mix}_{Z,AC_v} = 0 \qquad (3a)$$

and

$$\Delta G_{Z,BC_v} + \overline{\Delta G}^{mix}_{Z,BC_v} = 0 \qquad (3b)$$

$\Delta G_{Z,AC_v}$ and $\Delta G_{Z,BC_v}$ are the free enthalpies of disproportionation of the binary phase AC_u and AC_v according to:

$$(w-u)A(B)C_u \longrightarrow (w-v)\,A(B)C_u + (v-u)A(B)C_w \ldots . \Delta G_{Z,A(B)C_v}$$

and the $\overline{\Delta G}^{mix}_{Z,A(B)C_v}$ abbreviates the sum of mixing terms according to the same reaction scheme.

The obvious meaning of equations (3a) and (3b) is that the free enthalpies of disproportionation of the binary phases are, under equilibrium conditions, exactly counterbalanced by the free energies of mixing in the three phase-solutions. Any deviation from equilibrium will result in the appearance of a finite quantity, ϕ_Z, on the right hand side of equations (3), which, in essence, is a measure of the imbalance between the disproportionation terms for the binary phases and the mixing quantities. Generalizing conditions (3), we may write therefore:

$$\phi_{Z(A)} = \Delta G_{Z,AC_v} + \overline{\Delta G}^{mix}_{Z,AC_v} \qquad (4a)$$

$$\phi_{Z(B)} = \Delta G_{Z,BC_v} + \overline{\Delta G}^{mix}_{Z,BC_v} \qquad (4b)$$

We note that at equilibrium, $\phi_Z(x) = 0$; when $\phi_Z(x)$ assumes positive values, the solution $(A,B)C_v$ is stable, whereas for $\phi_Z(x) < 0$, single phase solutions of $(A,B)C_v$ become unstable.

The integral free enthalpy of disproportionation, $\phi_Z(x'')$ of the solid solution $(A,B)C_v$ is given by:

$$\phi_Z(x'') = x''_A \cdot \phi_{Z(A)} + x''_B \cdot \phi_{Z(B)} \qquad (5)$$

It can be shown[24], and in view of its importance, the mathematical proof is given in the appendix, that both functions, $\phi_{Z(A)}$ and $\phi_{Z(B)}$, are identical, and additionally, since $x''_A = 1-x''_B$, are equal to the integral free enthalpy of disproportionation of the ternary phase solution $(A,B)C_v$, viz.,

$$\phi_Z(x'') \equiv \phi_{Z(A)} \equiv \phi_{Z(B)} \qquad (6)$$

We arrive, therefore, at the interesting result that the relative stability of the ternary phase solution is uniquely defined by the partial free enthalpies of disproportionation of either phase, as calculated from either equations 4(a) or 4(b). We also, note that equation (5) satisfies the following boundary conditions:

$$\phi_Z\left[x''_A = 1, \text{ or } x''_B = 0\right] = \Delta G_{Z,AC_v} \qquad (7a)$$

and

$$\phi_Z\left[x''_A = 0, \text{ or } x''_B = 1\right] = \Delta G_{Z,BC_v} \qquad (7b)$$

In order to evaluate the above relations quantitatively, we have to insert the free energies of the boundary phases as well as the mixing quantities of the ternary phase solutions.

From data compiled by E.K. Storms[25], H.L. Schick[26], and Y.A. Chang[27], as well as from values back-calculated from ternary phase diagrams[28, 29, 30]; we obtained the data listed in Table 3 for the tantalum carbides after linearization of some of the expressions. For the molybdenum

Table 3. Free Enthalpy Data of Tantalum Carbides (T > 1500°C).

Phase	Free Enthalpy of Formation of Reaction (cal/gr.-At. Ta)
TaC	$\Delta G_{f,TaC} = -35{,}300 - 1.80 \cdot T \log T + 6.48 \cdot T$
$TaC_{0.71}$	$\Delta G_{f,TaC_{0.71}} = -26{,}200 - 1.20 \cdot T$
Disproportionation of Ta_2C:	$\Delta G_{Z,TaC_{1/2}} = 1420 + 0.40 \cdot T$
$TaC_{1/2} \rightarrow 0.70\ TaC_{0.71} + 0.30\ Ta$	

carbides[8, 31], the data presented in Table 4 were used as the basis for the calculations.

As no data for the mixing quantities are available, the phase solutions are, for the sake of simplicity, assumed to behave ideally. The order-disorder transitions in the Me_2C-phases, as well as the occurrence of the ζ-phase in the ternary will also be disregarded in the calculations, since their effect upon the gross-equilibria in the system is only minor.

Choosing the mole fractions of molybdenum in the metal sublattices, i.e., x' for the (Ta, Mo)-ss, x'' for the $(Ta, Mo)_2C$-ss, and x''' for the $(Ta, Mo)C_{1-x}$-ss, as the concentration variable and inserting the thermodynamic data from Tables (3) and (4), we obtain the following expressions for the tie line distribution within the three, two-phase fields:

Table 4. Free Enthalpy Data of Molybdenum Carbides ($T > 1500°C$).

Phase	Free Enthalpy of Formation (cal/gr.-At. Mo)
$MoC_{\sim 1/2}$	$\Delta G_f = -4,760 - 1.36 \cdot T$
η-MoC_{1-x} ($1-x \sim 0.64$)	$\Delta G_f = -4,120 - 1.69 \cdot T$
α-MoC_{1-x} ($1-x \sim 0.70$)	$\Delta G_f = -2,200 - 2.55 \cdot T$

1. Two-phase equilibrium (Ta, Mo) + (Ta, Mo)$C_{\sim 1/2}$ ($u \simeq 0$; $v \simeq 1/2$):

$$\log K_{1,2} = \frac{3260}{T} - 0.037, \qquad (8)$$

where $K_{1,2}$ stands for

$$K_{1,2} = \frac{x'}{1-x'} \cdot \frac{1-x''}{x''}$$

2. Two-phase equilibrium (Ta, Mo) (Ta, Mo)$C_{\sim 0.71}$ ($u \simeq 0$, $w \simeq 0.71$):

$$\log K_{1,3} = \frac{5250}{T} - 0.295 \qquad (9)$$

3. Two-phase equilibrium (Ta, Mo)$C_{\sim 1/2}$-(Ta, Mo)$C_{0.71}$ ($v \simeq 1/2$, $w \simeq 0.71$):

$$\log K_{2,3} = \log \frac{K_{1,3}}{K_{1,2}} = \frac{1990}{T} - 0.258 \qquad (10)$$

$$K_{2,3} = \frac{x''}{1-x''} \cdot \frac{1-x'''}{x'''}$$

Gradients of the free enthalpies of the three solid solutions, from which the coexisting compositions between any two phase combinations can also be obtained from the horizontal intercepts (gradient = const), have been calculated for a number of temperatures and are shown in Figures 35(a) through 35(c).

Expanding equations 4(a) and 4(b) and inserting the stoichiometry factors, $u \simeq 0$, $v \simeq 1/2$, and $w \simeq 0.71$, we obtain the following expressions for the integral free enthalpy of disproportionation of the subcarbide phase into mixtures of metal and monocarbide solid solutions:

$$\phi_{Z(x'')} = \phi_{Z(Ta)} = \Delta G_{Z,\,TaC_{1/2}} + RT \ln \frac{x'''^{0.70}_{(Ta)} \cdot x'^{0.30}_{(Ta)}}{x''_{(Ta)}} \qquad (11)$$

or the equivalent expression applying to Mo_2C:

$$\phi_{Z(x'')} = \phi_{Z(Mo)} = \Delta G_{Z,\,MoC_{1/2}} + RT \ln \frac{x'''^{0.70}_{(Mo)} \cdot x'^{0.30}_{(Mo)}}{x''_{(Mo)}} \qquad (12)$$

The equilibrium compositions of the metal and monocarbide solid solutions, i.e., x' and x''', can be obtained graphically from the gradient curves [Figures 35(a) through 35(c)], or can be calculated from equations 8, 9, and 10, for a series of preselected subcarbide compositions, x''; $\phi_Z(x'')$ is then computed from equation (11) or (12).

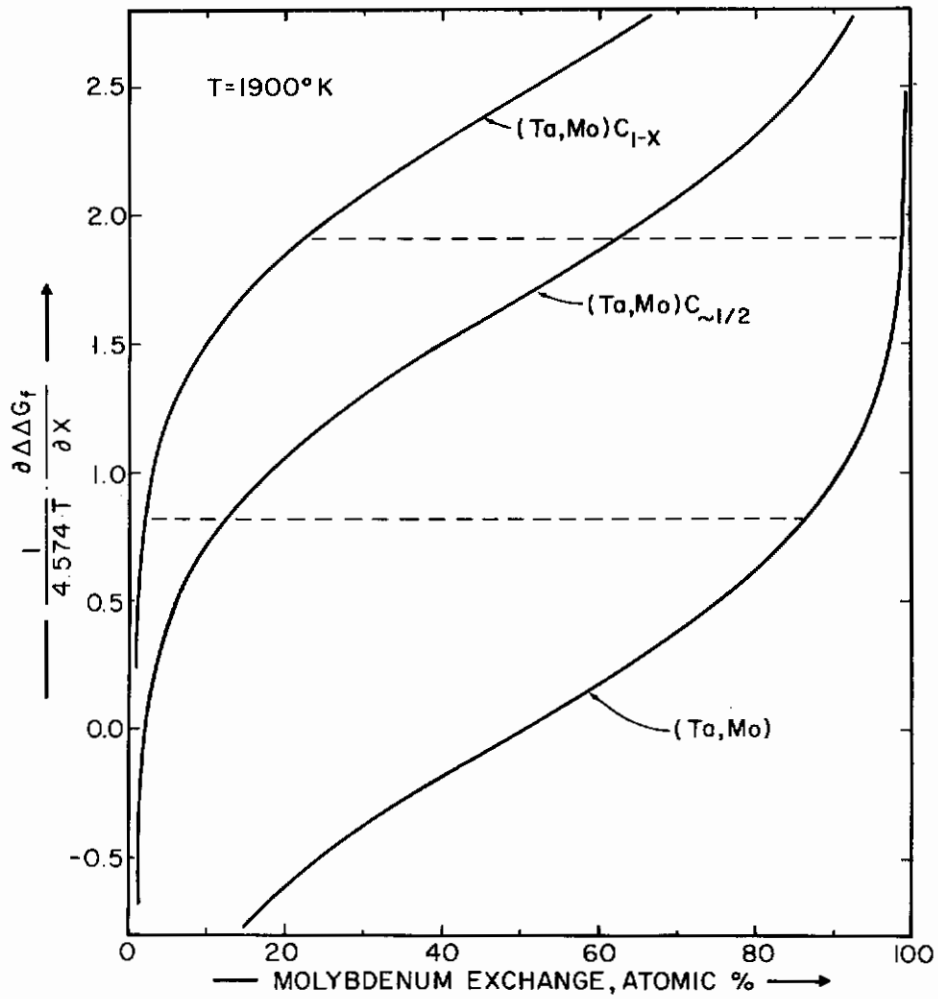

Figure 35(a)

Figures 35(a) through 35(c).

Free Enthalpy-Concentration Gradients for (Ta, Mo) and for Tantalum-Molybdenum Carbide Solid Solutions.

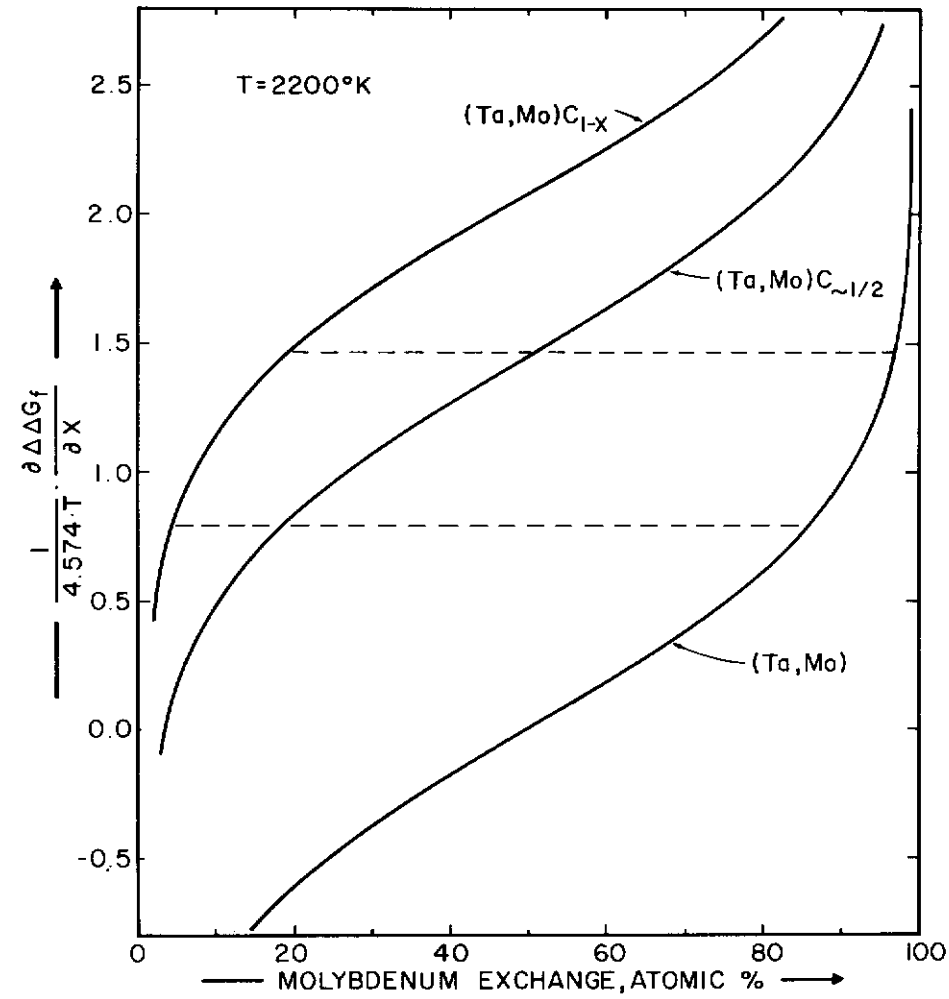

Figure 35(b)

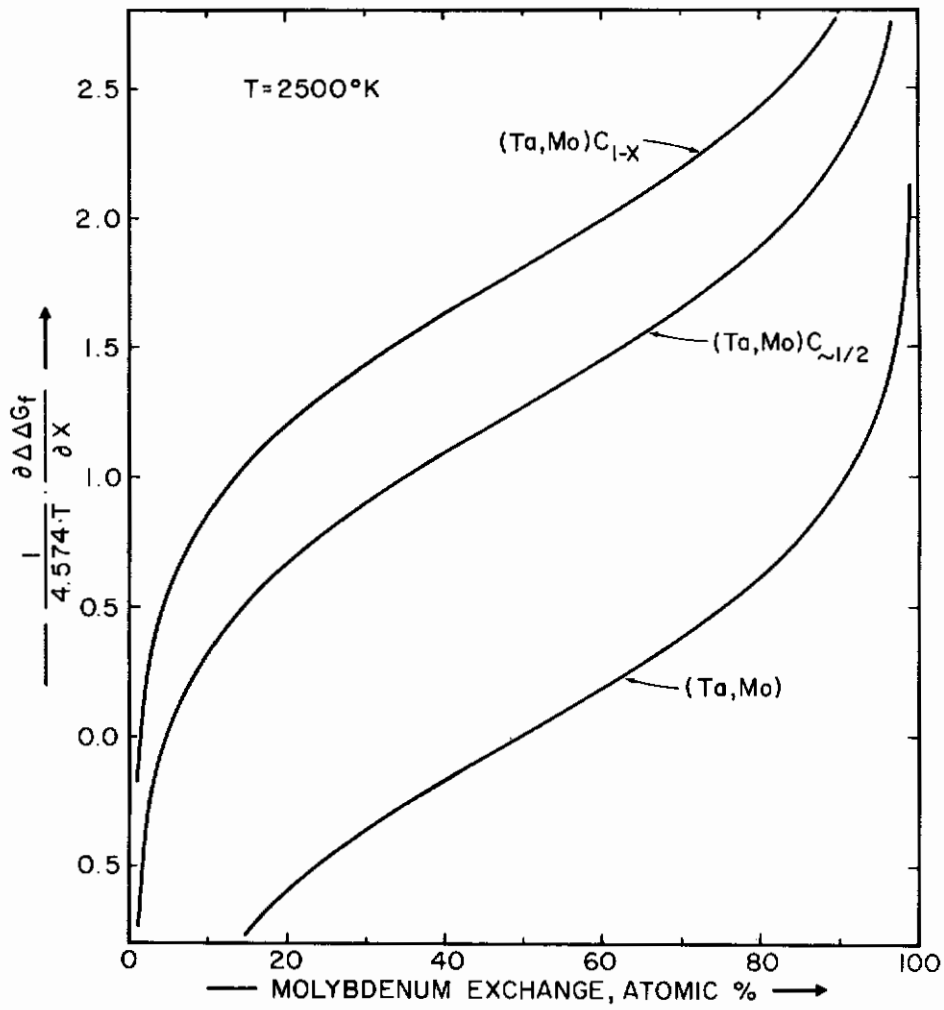

Figure 35(c).

Carrying out the detailed calculations, we obtained the data shown in Figure 36 for the integral free enthalpy of disproportionation of the subcarbide. In this figure, the ordinate values of 0 and 100 At% Mo correspond, by definition, to the free enthalpies of disproportionation of the boundary phases $TaC_{\sim 1/2}$ and $MoC_{1/2}$.

One can see by comparing the data in Figure 36 with the experimental solubilities at the respective temperatures that the actual phase behavior is reproduced very well, especially considering the fact that ideal solution behavior has been assumed in the calculations, and that the thermodynamic data are probably also not overly accurate. The calculated critical solution point at 37 At% Mo and 2470°k (~2200°C) also compares favorably with the experimental values of ~40 At% Mo and 2230°C.

The remaining equilibria to be considered in the system, namely, the three-phase equilibria (Ta, Mo)C_{1-x}-ss + η -MoC_{1-x}-ss + C, (Ta, Mo)C_{1-x}-ss + (Ta, Mo)$_2$C-ss + η-MoC_{1-x}-ss, and (Ta, Mo)C_{1-x}-ss + (Ta, Mo)$_2$C-ss + C, can be calculated in the same manner as shown for the more complex equilibria in the metal-rich region of the system. Since these calculations are simple, but lengthy, they will be omitted.

With the vertices of the three-phase equilibria known, the ternary region can be subdivided and the tie lines inserted into the resulting two-phase ranges. Three such temperature sections, at 1900°K, 2200°K, and 2470°K, have been calculated and are shown in Figures 37(a) through 37(c).

In the simplified approach, only the relative metal exchanges are obtained from the calculations, and therefore no specific description of the contours of the single-phase boundaries is possible; these boundaries, therefore, are shown as straight lines originating from the respective binary phase boundaries and terminating at the calculated metal exchange of the vertices of the three-phase equilibria.

Comparing the data obtained for the Ta-Mo-C system with previous, analogous calculations carried out for Ta-W-C[4] and Nb-Mo-C[5] alloys, it

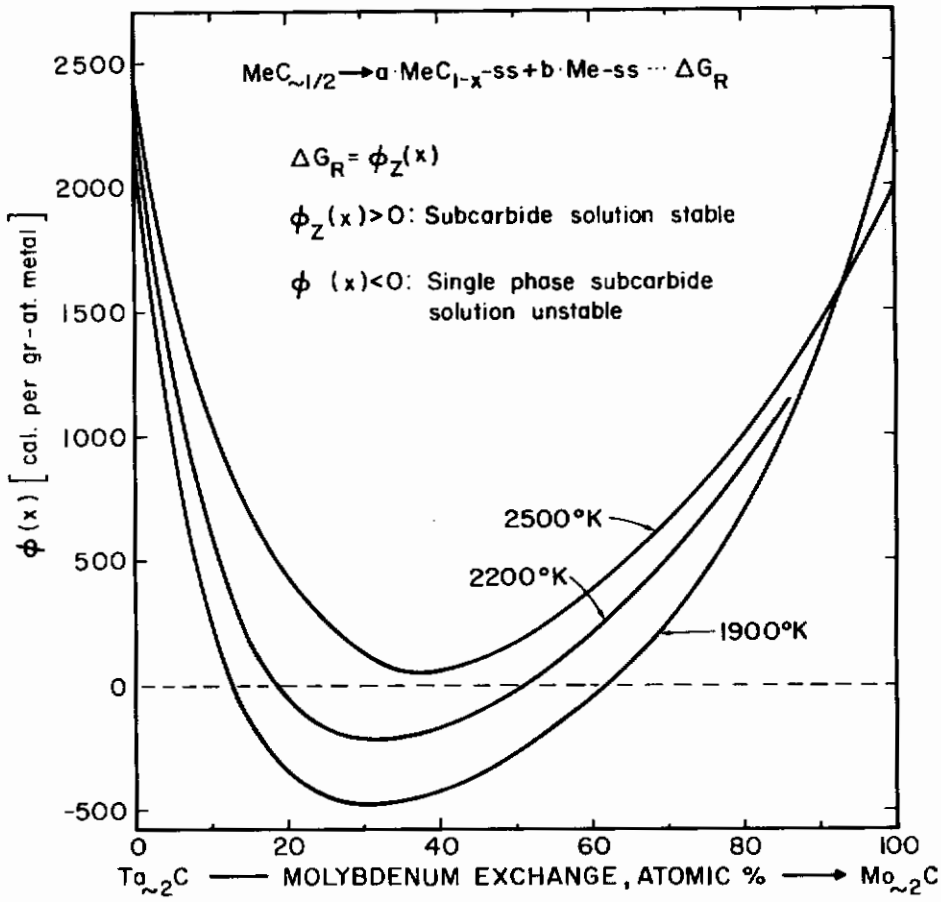

Figure 36. Calculated Integral Free Enthalpy of Disproportionation of the $(Ta, Mo)_2C$ Solid Solution into Solutions of Metal Alloy, (Ta, Mo), and Monocarbide, $(Ta, Mo)C_{1-x}$.

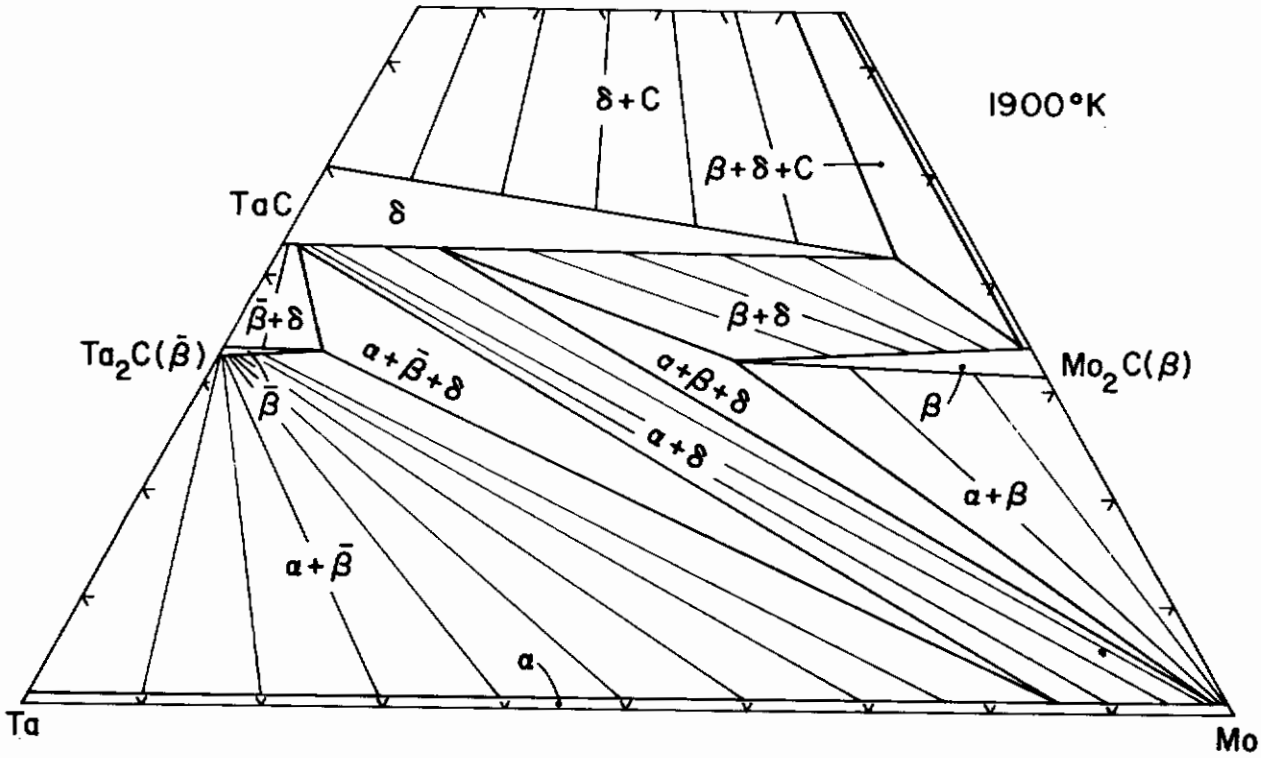

Figure 37(a).

Figures 37(a) through 37(c):

Calculated Temperature Sections for the Ta-Mo-C System.

37(a). 1900°K
37(b). 2200°K
37(c). 2470°K

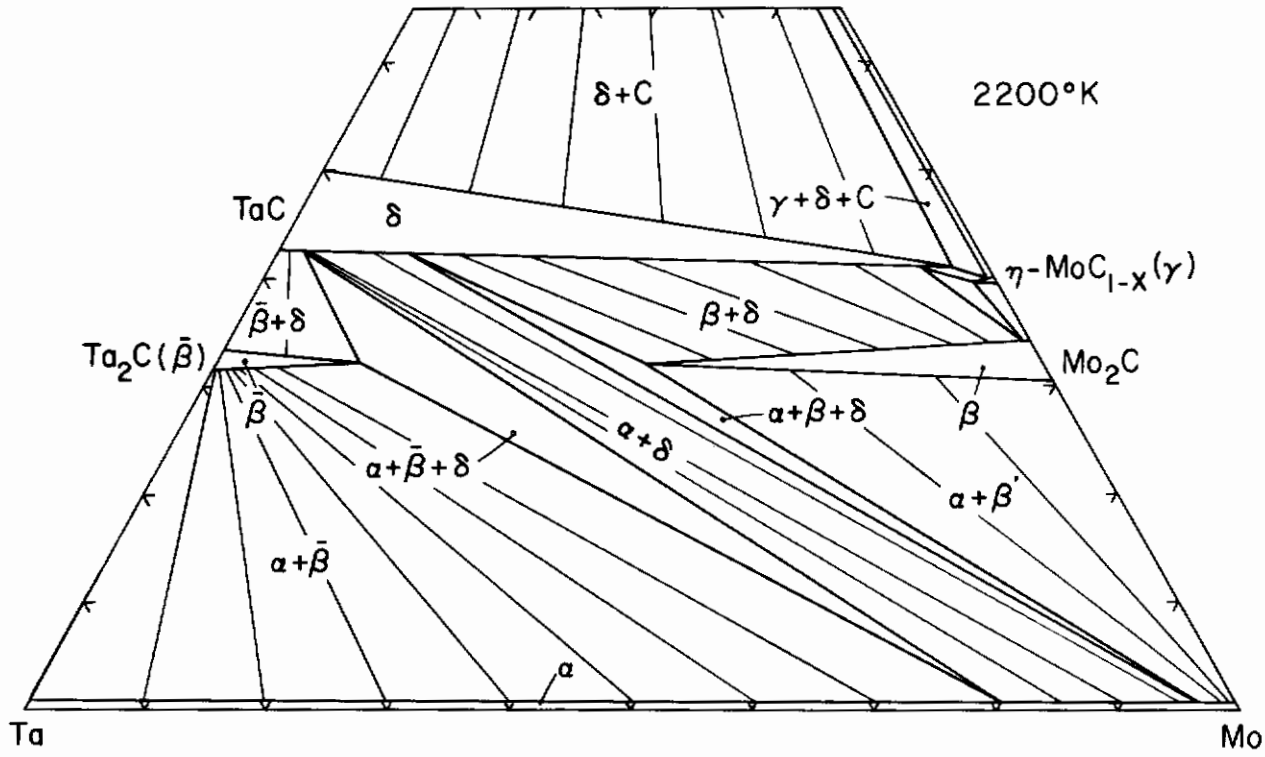

Figure 37(b).

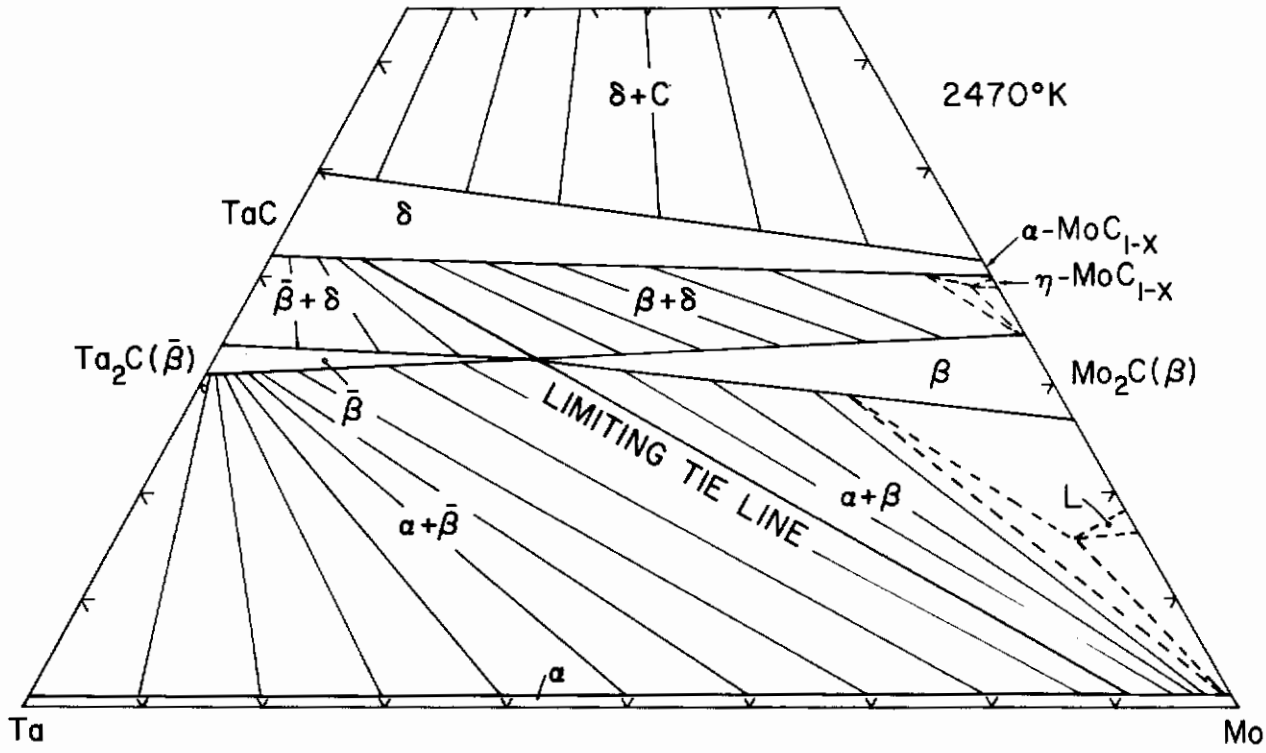

Figure 37(c).

is seen that the reason for the formation of a complete solid solution in the tantalum-containing systems is mainly due to the somewhat higher relative stability of Ta_2C as compared to Nb_2C. In addition, the interruption of the subcarbide solid solution by an equilibrium between monocarbide and metal is aided by the large stability differences between the group V and group VI metal carbides. This causes the tie lines to assume extreme positions in the two-phase fields. This relationship is immediately expressed by the fact, that the somewhat higher stability of the molybdenum carbides, as compared to tungsten carbides, causes a lower critical temperature in the Ta-Mo-C system than in the Ta-W-C system. This behavior also explains the complete solid solution formation of the subcarbides in the corresponding systems with vanadium at low temperatures, for the vanadium carbides have the lowest stability among the group V metal carbides.

VI. NOTES TO THE TECHNICAL APPLICABILITY OF Ta-Mo-C ALLOYS

Among phase diagram features which could be of interest in the technical application of Ta-Mo-C-based alloys, the disproportionation reaction of the $(Ta, Mo)_2C$ solid solution might offer possibilities for the development of composites or cutting tools having a controlled, ultrafine distribution of the phases. As an example, it is well-known in the cutting tool field that a fine grain size of the abrasive component (carbide) is necessary to achieve higher strength and better cutting performance. Present technology uses practically exclusively mechanical milling techniques to comminute the carbides. Apart from undesirable changes as a result of increased contamination by prolonged milling, grain sizes smaller than one micron are difficult to achieve by mechanical means; binder-induced grain growth during fabrication poses an additional problem. On the other hand, by using metallurgical reactions, such as, for example, the decomposition of the $(Ta, Mo)_2C$ solid solution, structures with almost any degree of dispersion of the constituent phases can be achieved by appropriate selection of annealing conditions.

Considering the phase conditions existing for $(Ta, Mo)_2C$ and $(Ta, W)_2C$, one has an example of a reversible reaction leading to a self-reinforced composite in the critical temperature range: At low temperatures, where the

carbide phase is very brittle and thus sensitive to mechanically or thermally induced stresses, the alloy consists of a two-phase structure of metal and monocarbide; at high temperatures, where the carbide phase is sufficiently ductile to relieve stresses, the alloy consists of a single-phased, refractory carbide.

Although it is quite likely that three-component alloys based on the combinations Ta-W-C or Ta-Mo-C may not satisfy specific application needs, it is possible to adjust the alloy properties by further alloying. Further improvement of the mechanical behavior may be achieved by adding semi-inert binder materials, such as alloys based on the metals from the iron-group.

VII. SUMMARY

The phase relationships in the ternary alloy system tantalum-molybdenum-carbon are summarized as follows:

Above 1960°C, the cubic (B1) monocarbides TaC_{1-x} and α-MoC_{1-x} form a continuous series of solid solutions; melting of the ternary solid solution occurs over the entire concentration range according to the maximum-type. Below 1960°C, the molybdenum exchange in tantalum monocarbide is temperature-dependent and decreases to approximately 70-73 At% at 1500°C. The course of the lattice parameters show a slight positive deviation from a linear relationship.

Above 2230°C, Ta_2C and Mo_2C form a continuous series of solid solutions. For compositions up to ~90 Mole% Mo_2C, melting occurs under disproportionation, while alloys between 90 to 100 Mole% Mo_2C melt according to the maximum type. At 2230°C, the subcarbide solid solution disproportionates in a pseudobinary, eutectoid reaction into metal and monocarbide phase. The critical concentration lies at 40 Mole% Mo_2C.

Towards lower temperatures, the mutual metal exchange in both subcarbides is temperature-dependent, and amounts to 8 Mole% Mo_2C in Ta_2C, and 34 Mole% Ta_2C in Mo_2C at 1500°C. Both solutions are restricted by

three-phase equilibria towards the ternary phase field. The sublattice order-disorder transformation temperatures in both subcarbides are lowered by the mutual metal exchange.

The ternary range of the η-MoC_{1-x} phase is very restricted. The ζ-phase, which is metastable in the binary tantalum-carbon system, is stabilized by small molybdenum additions and forms equilibria with the monocarbide, subcarbide, and the metal phase.

Seven isothermal reactions occur in the system in the range from melting to 1500°C. There are one each of a Class I, Class II, and Class III ternary reaction, and four isotherms correspond to limiting tie lines. These reaction isotherms, in order of decreasing temperatures, are:

1. 2540°C: $L \longrightarrow$ (Ta, Mo_2C-ss

2. 2520°C: $L + Bl\text{-ss } (\delta) \longrightarrow \eta\text{-}MoC_{1-x}\text{-ss } (\gamma) + (Ta, Mo)_2C\ (\beta)$

3. 2230°C: $(Ta, Mo)_2C\text{-ss } (\beta) \longrightarrow (Ta, Mo)\text{-ss } (\alpha) + (Ta, Mo)C_{1-x}\text{-ss } (\delta)$

4. ~2080°C: Limiting Tie Line,

   $(Ta, Mo)_2C$-ss(β'') disordered, C-rich + $(Ta, Mo)_2C$-ss($\bar{\gamma}$), ordered +

   + $(Ta, Mo)C_{1-x}$-ss (δ).

5. ~2050°C: (Ta, Mo)-ss(α) + $(Ta, Mo)_2C$-ss($\bar{\beta}'$), disordered + $(Ta, Mo)C_{1-x}$-ss(δ) $\rightarrow \zeta$

6. ~1980°C: $(Ta, Mo)_2C$-ss($\bar{\beta}''$) $\rightarrow (Ta, Mo)_2C$-ss($\bar{\beta}$), ordered + $(Ta, Mo)C_{1-x}$ (δ)

7. ~1550°C: η-MoC_{1-x}-ss(γ) $\rightarrow (Ta, Mo)C_{1-x}$-ss ($\delta$) + $(Ta, Mo)_2C$-ss ($\bar{\beta}$) + C

Two further reaction isotherms, a limiting tie line and a Class II four-phase reaction are indicated in the range from 1400-1500°C as a result of the order-disorder transformation in Mo_2C.

Based on existing thermochemical data for the binary metal carbides, the phase relationships in the Ta-Mo-C system were thermodynamically analyzed; good agreement was obtained between the calculated and experimental phase equilibria.

REFERENCES

1. Work conducted under U.S. Air Force Contract AF 33(615)-1249. Report Series AFML-TR-65-2, Part I-IV (32 Volumes, 1964 to 1967).

2. E. Rudy, F. Benesovsky, and K. Sedlatchek: Mh.Chem. 92 (1961), 841.

3. E. Rudy, El. Rudy, and F. Benesovsky: Mh.Chem. 93 (1962), 1176

4. E. Rudy: Techn. Report AFML-TR-65-2, Part II, Vol. VIII (March 1966).

5. E. Rudy, C.E. Brukl, and St. Windisch: Techn. Doc. Report AFML-TR-65-2, Part II, Vol. XV (March 1967; Trans. AIME (in press).

6. H. Bückle: Z. Metallkde 37 (1946), 53

7. G.A. Geach and D. Summers-Smith: J. Inst. Metals 80 (1951-1952), 143.

8. E. Rudy, St. Windisch, A.J. Stosick, and J.R. Hoffman: Techn. Doc. Report AFML-TR-65-2, Part I, Vol. XI (April 1967), Trans. AIME (in press).

9. E. Parthe and V. Sadagopan: Acta Cryst. 16 (1963), 202.

10. H. Nowotny, E. Parthe, R. Kieffer, and F. Benesovsky: Mh.Chem. 85 (1954), 255.

11. A.L. Bowman, T.C. Wallace, J.L. Yarnell, R.G. Wenzel, and E.K. Storms: Acta Cryst. 19 (1965), 6

12. E. Rudy and D.P. Harmon: Tech. Doc. Report, AFML-TR-65-2, Part I, Vol. V. (Jan. 1966).

13. R. Lesser and G. Brauer: Z. Metallkde 49 (1958), 622.

14. I. Zaplatynsky: J. Amer. Ceram. Soc. 49, No.2 (1966), 109.

15. W.F. Brizes and S.M. Tobin: J. Am. Ceram. Soc. 50 (1967), 115

16. H. Nowotny and R. Kieffer: Metallforschung 2 (1947), 257

17. Unpublished work by E. Rudy, El. Rudy, and F. Benesovsky, quoted in E. Rudy and Y.A. Chang: Proceedings of the Vth Plansee Seminar, 1964, 786 (Editor, F. Benesovsky, published by Springer, Wien, 1965).

18. W.B. Pearson: Handbook of Lattice Spacings and Structures of Metals and Alloys (Pergamon Press, 1958).

19. E. Rudy, St. Windisch, and Y.A. Chang: Techn. Doc. Report AFML-TR-65-2, Part I, Vol. I (Dec. 1964).

REFERENCES (cont.)

20. E. Rudy and G. Progulski: Planseeberichte f. Pulvermetallurgie 15 (1967), 13-45, Techn. Doc. Rept. AFML-TR-65-2, Part III, Vol. II (Sept. 1966).

21. M. Pirani and H. Alterthum: Z. Elektrochemie 29 (1923).

22. E. Rudy, St. Windisch, and C.E. Brukl: AFML-TR-65-2, Part I, Vol. XII (July 1967) Planseeber. Pulvermet. 1967 (in press).

23. E. Rudy: Part I, Z. Metallkde 54 (1963), 112-122, Part II, Z.Metallkde. 54 (1963), 213-223.

24. E. Rudy: U.S. Air Force Contract AF 33(615)-1249, Part IV, Vol. II (Jan. 1966).

25. E.K. Storms: Refractory Carbides (Academic Press, 1967, in press).

26. H.L. Schick: Thermodynamics of Certain Refractory Compounds, Vol.II (Academic Press, 1966).

27. Y.A. Chang: U.S. Air Force Contract AF 33(615)-1249, Tech. Doc. Report, AFML-TR-65-2, Part IV, Vol. I (Sept. 1965).

28. E. Rudy, El. Rudy, and F. Benesovsky: Mh.Chem. 93 (1962), 1776

29. E. Rudy and Y.A. Chang: Proceedings of the Vth Plansee Seminar, 1964, 786 (Editor F. Benesovsky, Wien, Springer, 1965).

30. E. Rudy and H. Nowotny: Mh. Chem. 94 (1963), 508

31. L.B. Pankratz, W.W. Weller, and E.G. King: U.S. Bureau of Mines Report of Investigations No. 6861 (1966).

APPENDIX

Proof of the Identity of the Function $\phi_{Z(A)}$ and $\phi_{Z(B)}$.

By definition (T, p = const):

$$\phi_{Z(A)} = \Delta G_{Z, AC_v} + \overline{\Delta G}^{mix}_{Z, AC_v} \qquad (1a)$$

$$\phi_{Z(B)} = \Delta G_{Z, BC_v} + \overline{\Delta G}^{mix}_{Z, BC_v}, \qquad (2a)$$

with

$$\Delta G_{Z, AC_v} = (w-v)\, \Delta G_{f, AC_u} + (v-u)\, \Delta G_{f, AC_w} - (w-u)\, \Delta G_{f, AC_v} \qquad (3a)$$

and

$$\Delta G_{Z, BC_v} = (w-v)\, \Delta G_{f, BC_u} + (v-u)\, \Delta G_{f, BC_w} - (w-u)\, \Delta G_{f, BC_v} \qquad (4a)$$

$\Delta G_{f, i}$ ..... Free enthalpy of formation of phase i, per grammatom (A, B)

The integral mixing terms for the three phase solutions shall be given by:

$$\Delta G^{mix}_{(A, B)C_u} = \phi_{1m}(x'_A); \qquad (x'_A + x'_B) = 1$$

$$\Delta G^{mix}_{(A, B)C_v} = \phi_{2m}(x''_A); \qquad (x''_A + x''_B) = 1$$

$$\Delta G^{mix}_{(A, B)C_w} = \phi_{3m}(x'''_A); \qquad (x'''_A + x'''_B) = 1$$

The partial quantities $\overline{\Delta G}^{mix}$ are related to the integral terms by:

$$\overline{\Delta G}^{mix}_{A_{(u)}} = \phi_{1m} + x'_B \cdot \frac{\partial \phi_{1m}}{\partial x'_A} \tag{5a}$$

$$\overline{\Delta G}^{mix}_{A_{(v)}} = \phi_{2m} + x''_B \cdot \frac{\partial \phi_{2m}}{\partial x''_B} \tag{6a}$$

$$\overline{\Delta G}^{mix}_{A_{(w)}} = \phi_{3m} + x'''_B \cdot \frac{\partial \phi_{3m}}{\partial x'''_A} \tag{7a}$$

Using these expressions, the partial mixing quantities, $\overline{\Delta G}^{mix}_{Z}$, in equations (1a) and (1b) become:

$$\overline{\Delta G}^{mix}_{Z, AC_v} = (v-u)\,\overline{\Delta G}^{mix}_{A_{(w)}} + (w-v)\,\overline{\Delta G}^{mix}_{A_{(u)}} - (w-u)\,\overline{\Delta G}^{mix}_{A_{(v)}}$$

$$= (v-u)\,\phi_{3m} + (w-v)\,\phi_{1m} - (w-u)\,\phi_{2m} + (v-u)\,x'''_B \frac{\partial \phi_{3m}}{\partial x'''_A} +$$

$$+ (w-v)\,x'_B \frac{\partial \phi_{1m}}{\partial x'_A} - (w-u)\,x''_B \frac{\partial \phi_{2m}}{\partial x''_A} \tag{8a}$$

The analogous calculation for the component B yields:

$$\overline{\Delta G}^{mix}_{Z, BC_v} = (v-u)\,\phi_{3m} + (w-v)\,\phi_{1m} - (w-u)\,\phi_{2m} + (v-u)\,x'''_A \frac{\partial \phi_{3m}}{\partial x'''_B} +$$

$$+ (w-v)\,x'_A \frac{\partial \phi_{1m}}{\partial x'_B} - (w-u)\,x''_A \frac{\partial \phi_{2m}}{\partial x''_B} \tag{9a}$$

The conditional equation for the three, two-phase equilibria possible between the phases $(A,B)C_u$, $(A,B)C_v$, and $(A,B)C_w$ is given by:

$$\left[\frac{\partial \Delta G_{f,(A,B)C_u}}{\partial x'}\right]_{T,p} = \left[\frac{\partial \Delta G_{f,(A,B)C_v}}{\partial x''}\right]_{T,p} = \left[\frac{\partial \Delta G_{f,(A,B)C_w}}{\partial x'''}\right]_{T,p}, \quad (10a)$$

where

$$\Delta G_{f,(A,B)C_u} = x'_A \Delta G_{f,AC_u} + x'_B \Delta G_{f,BC_u} + \phi_{1m}$$

$$\Delta G_{f,(A,B)C_u} = x''_A \Delta G_{f,AC_v} + x''_B \Delta G_{f,BC_v} + \phi_{2m}$$

$$\Delta G_{f,(A,B)C_w} = x'''_A \Delta G_{f,AC_w} + x'''_B \Delta G_{f,BC_w} + \phi_{3m}$$

Differentiation and rearrangement of the terms immediately yields:

$$\Delta G_{f,AC_u} - \Delta G_{f,GC_u} + \frac{\partial \phi_{1m}}{\partial x'_A} = \Delta G_{f,AC_v} - \Delta G_{f,BC_v} + \frac{\partial \phi_{2m}}{\partial x''_A} \quad (11a)$$

and

$$\Delta G_{f,AC_v} - \Delta G_{f,BC_v} + \frac{\partial \phi_{2m}}{\partial x''_A} = \Delta G_{f,AC_w} - \Delta G_{f,BC_w} + \frac{\partial \phi_{3m}}{\partial x'''_A} \quad (12a)$$

Combining equations (1a) and (2a) with (8a) and (9a), and rearranging the terms, we obtain:

$$\phi_{Z(A)} - \phi_{Z(B)} = \Delta G_{Z,AC_v} - \Delta G_{Z,BC_v} + (v-u)\frac{\partial \phi_{3m}}{\partial x'''_A} + (w-v)\frac{\partial \phi_{1m}}{\partial x'_A} - (w-u)\frac{\partial \phi_{2m}}{\partial x''_A} \quad (13a)$$

Substitution for $\frac{\partial \phi_{2m}}{\partial x''_A}$ and $\frac{\partial \phi_{3m}}{\partial x'''_A}$ from equations (11a) and (12a) yields:

$$\begin{aligned}\phi_{Z(A)} - \phi_{Z(B)} = {} & \Delta G_{Z,AC_v} - \Delta G_{Z,BC_v} + (v-u)\left[\Delta G_{f,AC_u} - \Delta G_{f,BC_u} - \right. \\ & \left. - \Delta G_{f,AC_w} + \Delta G_{f,BC_w}\right] - (w-u)\left[\Delta G_{f,AC_u} - \Delta G_{f,BC_u} - \right. \\ & \left. - \Delta G_{f,AC_v} + \Delta G_{f,BC_v}\right] \end{aligned} \quad (14a)$$

From relations (3a) and (4a) immediately follows that the last two terms in equation (14a) are equal to $\Delta G_{Z,BC_v} - \Delta G_{Z,AC_v}$; hence,

$$\phi_{Z(A)} - \phi_{Z(B)} = 0$$

or

$$\underline{\phi_{Z(A)} = \phi_{Z(B)}}$$

i.e., both quantities, $\phi_{Z(A)}$ and $\phi_{Z(B)}$, are equal, independent of the solution behavior.

UNCLASSIFIED

Security Classification

DOCUMENT CONTROL DATA - R&D

(Security classification of title, body of abstract and indexing annotation must be entered when the overall report is classified)

1. ORIGINATING ACTIVITY *(Corporate author)* Aerojet-General Corporation Materials Research Laboratory Sacramento, California	2a. REPORT SECURITY CLASSIFICATION Unclassified 2b. GROUP N.A.

3. REPORT TITLE

Ternary Phase Equilibria in Transition Metal-Boron-Carbon-Silicon Systems

Part II. Ternary Systems; Volume XVII. Constitution of Ternary Ta-Mo-C Alloys

4. DESCRIPTIVE NOTES *(Type of report and inclusive dates)*

5. AUTHOR(S) *(Last name, first name, initial)*

E. Rudy
St. Windisch
C. E. Brukl

6. REPORT DATE	7a. TOTAL NO. OF PAGES	7b. NO. OF REFS
December 1967	71	31

8a. CONTRACT OR GRANT NO.	9a. ORIGINATOR'S REPORT NUMBER(S)
AF 33(615)-1249 b. PROJECT NO. 7350 c. Task No. 735001 d.	9b. OTHER REPORT NO(S) *(Any other numbers that may be assigned this report)* AFML-TR-65-2, Part II, Vol. XVII

10. AVAILABILITY/LIMITATION NOTICES

Distribution of this document is unlimited. It may be released to the Clearinghouse, Department of Commerce, for sale to the General Public.

11. SUPPLEMENTARY NOTES	12. SPONSORING MILITARY ACTIVITY
	AFML (MAMC) Wright-Patterson AFB, Ohio 45433

13. ABSTRACT

The ternary system tantalum-molybdenum-carbon was investigated by means of X-ray, melting point, DTA, and metallographic techniques on chemically and thermally characterized specimens; a complete phase diagram for temperatures above 1500°C was established.

The observed phase relationships are thermodynamically analyzed and the calculated temperature sections are found to be in good agreement with the experimental observations.

DD FORM 1 JAN 64 1473

UNCLASSIFIED

Security Classification

14. KEY WORDS	LINK A		LINK B		LINK C	
	ROLE	WT	ROLE	WT	ROLE	WT
High Temperature Ternary Phase Equilibria Refractory Carbides Thermodynamics of Phase Reactions						

INSTRUCTIONS

1. ORIGINATING ACTIVITY: Enter the name and address of the contractor, subcontractor, grantee, Department of Defense activity or other organization *(corporate author)* issuing the report.

2a. REPORT SECURITY CLASSIFICATION: Enter the overall security classification of the report. Indicate whether "Restricted Data" is included. Marking is to be in accordance with appropriate security regulations.

2b. GROUP: Automatic downgrading is specified in DoD Directive 5200.10 and Armed Forces Industrial Manual. Enter the group number. Also, when applicable, show that optional markings have been used for Group 3 and Group 4 as authorized.

3. REPORT TITLE: Enter the complete report title in all capital letters. Titles in all cases should be unclassified. If a meaningful title cannot be selected without classification, show title classification in all capitals in parenthesis immediately following the title.

4. DESCRIPTIVE NOTES: If appropriate, enter the type of report, e.g., interim, progress, summary, annual, or final. Give the inclusive dates when a specific reporting period is covered.

5. AUTHOR(S): Enter the name(s) of author(s) as shown on or in the report. Enter last name, first name, middle initial. If military, show rank and branch of service. The name of the principal author is an absolute minimum requirement.

6. REPORT DATE: Enter the date of the report as day, month, year; or month, year. If more than one date appears on the report, use date of publication.

7a. TOTAL NUMBER OF PAGES: The total page count should follow normal pagination procedures, i.e., enter the number of pages containing information.

7b. NUMBER OF REFERENCES: Enter the total number of references cited in the report.

8a. CONTRACT OR GRANT NUMBER: If appropriate, enter the applicable number of the contract or grant under which the report was written.

8b, 8c, & 8d. PROJECT NUMBER: Enter the appropriate military department identification, such as project number, subproject number, system numbers, task number, etc.

9a. ORIGINATOR'S REPORT NUMBER(S): Enter the official report number by which the document will be identified and controlled by the originating activity. This number must be unique to this report.

9b. OTHER REPORT NUMBER(S): If the report has been assigned any other report numbers *(either by the originator or by the sponsor)*, also enter this number(s).

10. AVAILABILITY/LIMITATION NOTICES: Enter any limitations on further dissemination of the report, other than those imposed by security classification, using standard statements such as:

(1) "Qualified requesters may obtain copies of this report from DDC."

(2) "Foreign announcement and dissemination of this report by DDC is not authorized."

(3) "U. S. Government agencies may obtain copies of this report directly from DDC. Other qualified DDC users shall request through _____."

(4) "U. S. military agencies may obtain copies of this report directly from DDC. Other qualified users shall request through _____."

(5) "All distribution of this report is controlled. Qualified DDC users shall request through _____."

If the report has been furnished to the Office of Technical Services, Department of Commerce, for sale to the public, indicate this fact and enter the price, if known.

11. SUPPLEMENTARY NOTES: Use for additional explanatory notes.

12. SPONSORING MILITARY ACTIVITY: Enter the name of the departmental project office or laboratory sponsoring *(paying for)* the research and development. Include address.

13. ABSTRACT: Enter an abstract giving a brief and factual summary of the document indicative of the report, even though it may also appear elsewhere in the body of the technical report. If additional space is required, a continuation sheet shall be attached.

It is highly desirable that the abstract of classified reports be unclassified. Each paragraph of the abstract shall end with an indication of the military security classification of the information in the paragraph, represented as *(TS)*, *(S)*, *(C)*, or *(U)*.

There is no limitation on the length of the abstract. However, the suggested length is from 150 to 225 words.

14. KEY WORDS: Key words are technically meaningful terms or short phrases that characterize a report and may be used as index entries for cataloging the report. Key words must be selected so that no security classification is required. Identifiers, such as equipment model designation, trade name, military project code name, geographic location, may be used as key words but will be followed by an indication of technical context. The assignment of links, rules, and weights is optional.